Criswell T, Leskov K, Miyamoto S, Luo G and Boothman DA. (2003). *Oncogene*, **22,** 5813–5827.
Darvasi A. (1998). *Nat. Genet.*, **18,** 19–24.
Demant P. (1992). *Cancer Biol.*, **3,** 159–166.
Ewart-Toland A, Briassouli P, de Koning JP, Mao JH, Yuan J, Chan F, MacCarthy-Morrogh L, Ponder BA, Nagase H, Burn J, Ball S, Almeida M, Linardopoulos S and Balmain A. (2003). *Nat. Genet.*, **34,** 403–412.
Ghebranious N and Donehower LA. (1998). *Oncogene*, **17,** 3385–3400.
Gould KA and Dove WF. (1998). *Exp. Lung Res.*, **24,** 437–453.
Gunes C, Heuchel R, Georgiev O, Muller KH, Lichtlen P, Bluthmann H, Marino S, Aguzzi A and Schaffner W. (1998). *EMBO J.*, **17,** 2846–2854.
Hellsten E, Evans JP, Bernard DJ, Janne PA and Nussbaum RL. (2001). *Dev. Biol.*, **240,** 641–653.
Kammann M, Laufs J and Gronenborn B. (1989). *Nucleic Acids Res.*, **17,** 5404.
Koropatnick J, Leibbrandt M and Chrian MG. (1989). *Radiat. Res.*, **119,** 356–365.
Lander E and Kruglyak L. (1995). *Nat. Genet.*, **11,** 241–247.
Langmade SJ, Ravindra R, Daniels PJ and Andrews GK. (2000). *J. Biol. Chem.*, **275,** 34803–34809.
Lichtlen P and Schaffner W. (2001). *Bioessays*, **23,** 1010–1017.
Lichtlen P, Wang Y, Belser T, Georgiev O, Certa U, Sack R and Schaffner W. (2001). *Nucleic Acids Res.*, **29,** 1514–1523.
Little JB. (2000). *Carcinogenesis*, **21,** 397–404.
Macphee M, Chepenik KP, Liddell RA, Nelson KK, Siracusa LD and Buchberg AM. (1995). *Cell*, **81,** 957–966.
Matsumoto Y, Kosugi S, Shinbo T, Chou D, Ohashi M, Wakabayashi Y, Sakai K, Okumoto M, Mori N, Aizawa S, Niwa O and Kominami R. (1998). *Oncogene*, **16,** 2747–2754.
Nadeau JH. (2001). *Nat. Rev. Genet.*, **2,** 165–174.
Okano H, Saito Y, Miyazawa T, Shinbo T, Chou D, Kosugi S, Takahashi Y, Odani S, Niwa O and Kominami R. (1999). *Oncogene*, **18,** 6677–6683.
Ponder BAJ. (2001). *Nature*, **411,** 336–341.
Radtke F, Georgiev O, Muller HP, Brugnera E and Schaffner W. (1995). *Nucleic Acids Res.*, **23,** 2277–2286.
Radtke F, Heuchel R, Georgiev O, Hergersberg M, Gariglio M, Dembic Z and Schaffner W. (1993). *EMBO J.*, **12,** 1355–1362.
Ruivenkamp CA, van Wezel T, Zanon C, Stassen AP, Vlcek C, Csikos T, Klous AM, Tripodis N, Perrakis A, Boerrigter L, Groot PC, Lindeman J, Mooi WJ, Meijjer GA, Scholten G, Dauwerse H, Paces V, van Zandwijk N, van Ommen GJ and Demant P. (2002). *Nat. Genet.*, **31,** 295–300.
Saito Y, Ochiai Y, Kodama Y, Tamura Y, Togashi T, Kosugi-Okano H, Miyazawa T, Wakabayashi Y, Hatakeyama K, Wakana S, Niwa O and Kominami R. (2001). *Oncogene*, **20,** 5243–5247.
Sato H, Tamura Y, Ochiai Y, Kodama Y, Hatakeyama K, Niwa O and Kominami R. (2003). *Cancer Sci.*, **94,** 668–671.
Saydam N, Georgiev O, Nakano MY, Greber UF and Schaffner W. (2001). *J. Biol. Chem.*, **276,** 25487–25495.
Smirnova IV, Bittel DC, Ravindra R, Jiang H and Andrews GK. (2000). *J. Biol. Chem.*, **275,** 9377–9384.
Tamai KT, Gralla EB, Ellerby LM, Valentine JS and Thiele DJ. (1993). *Proc. Natl. Acad. Sci. USA*, **90,** 8013–8017.
Wade CM, Kulbokas III EJ, Kirby AW, Zody MC, Mullikin JC, Lander ES, Lindblad-Toh K and Daly MJ. (2002). *Nature*, **420,** 574–578.
Wakabayashi Y, Inoue J, Takahashi Y, Matsuki A, Kosugi-Okano H, Shinbo T, Mishima Y, Niwa O and Kominami R. (2003a). *Biochem. Biophys. Res. Commun.*, **301,** 598–603.
Wakabayashi Y, Watanabe H, Inoue J, Takeda N, Sakata J, Mishima Y, Hitomi J, Yamamoto T, Utsuyama M, Niwa O, Aizawa S and Kominami R. (2003b). *Nat. Immunol.*, **4,** 533–539.
Wang Y, Wimmer U, Lichtlen P, Inderbitzin D, Stieger B, Meier PJ, Hunziker L, Stallmach T, Forrer R, Rülicke T, Georgiev O and Schaffner W. (2004). *FASEB J.*, **18,** 1071–1079.
Wright AF and Hastie ND. (2001). *Genome Biol.*, **2,** COMMENT2007.1–COMMENT2007.8.
Zhang H, Palmer R, Gao X, Kreidberg J, Gerald W, Hsiao L, Jensen RV, Gullans SR and Haber DA. (2003). *Curr. Biol.*, **13,** 1625–1629.

RADIATION RESEARCH 163, 000–000 (2005)
0033-7587/05 $15.00

Comparison of Properties of Spontaneous and Radiation-Induced Mouse Thymic Lymphomas: Role of Trp53 and Radiation

Tomoyuki Kubota,[a] Yoshihiro Yoshikai,[a] Yasushi Tamura,[a] Yukio Mishima,[a,b] Yutaka Aoyagi,[a] Ohtsura Niwa[c] and Ryo Kominami[a,b,1]

[a] *Department of Molecular Genetics, Graduate School of Medical and Dental Sciences and* [b] *Center for Transdisciplinary Research, Niigata University, Asahimachi 1-757, Niigata 951-8122, Japan; and* [c] *Radiation Biology Center, Kyoto University, Yoshida-Konoecho, Sakyou-Ku, Kyoto 606-8315, Japan*

Kubota, T., Yoshikai, Y., Tamura, Y., Mishima, Y., Aoyagi, Y., Niwa, O. and Kominami, R. Comparison of Properties of Spontaneous and Radiation-Induced Mouse Thymic Lymphomas: Role of Trp53 and Radiation. ***Radiat. Res.*** **163, 000–000 (2005).**

Mouse thymic lymphomas are readily induced by radiation and also arise without irradiation when the mice are null in Trp53 functions. In the present study, spontaneous thymic lymphomas in *Trp53*$^{-/-}$ mice were compared to those arising in irradiated *Trp53*$^{+/-}$ mice, revealing three features characteristic of the spontaneous lymphomas. (1) *Mp53D2*, a *Trp53* modifier that affects the latent period of radiogenic thymic lymphomas in *Trp53*$^{+/-}$ mice, had no effect on the development of spontaneous lymphomas. (2) A sex difference in the latency was found. (3) A marked difference was noted in the frequency of allelic loss at the *Ikaros* gene on chromosome 11, encoding a transcription factor required for normal lymphocyte development and differentiation; 2% in the lymphomas of *Trp53*$^{-/-}$ mice and 78% in the radiogenic lymphomas of *Trp53*$^{+/-}$ mice, suggesting that loss of *Trp53* may reduce the requirement for the loss of *Ikaros* for lymphomagenesis. Furthermore, allelic loss analysis on chromosome 19 localized a region that may harbor an unknown tumor suppressor gene. These results suggest intricate steps of lymphomagenesis influenced by the presence or absence of *Trp53*. © 2005 by Radiation Research Society

INTRODUCTION

Ionizing radiation is an important environmental carcinogen. A variety of damages are induced by ionizing radiation; the most serious of these is DNA double-strand breaks (DSBs). Two pathways of DSB repair are known; homologous recombination and non-homologous end joining (NHEJ). NHEJ is error-prone; homologous recombination is also error-prone but much less so than NHEJ. Since NHEJ is a major pathway in nonproliferating mammalian cells, multiple DSBs in a cell may enhance the generation of chromosomal rearrangements and mutations (*1–3*). It has long been thought that such mutations induced during repair of DSBs are the main cause of radiation-induced cancer.

It is known that DSBs activate a variety of damage responses. The Trp53-dependent signaling pathway is one such damage response that plays a key role in cell cycle checkpoints and apoptosis (*3, 4*). Irradiation also activates other signaling pathways, including NF-κB (Nfkb), c-Jun, c-Fos and MTF1 (*5, 6*). These represent both pro- and antiproliferative signals and modulate both apoptosis and the repair process. The relative balance of radiation-induced signals can determine the fate of a cell. In addition to misrepair of DSBs, damage responses are now well recognized as being involved in radiation carcinogenesis.

Li-Fraumeni syndrome patients with *Trp53* mutations are susceptible to sarcomas and breast carcinoma, and their outcomes range from early aggressive cancer to disease-free survival (*7, 8*). This may reflect the presence of variant alleles of low penetrance in the human population that can modify the impact of a given mutation (*9–11*). Mice heterozygous for *Trp53*, a model of Li-Fraumeni syndrome, are susceptible to radiation-induced thymic lymphomas (*12, 13*). As deduced from Li-Fraumeni syndrome cases, there is a strain dependence of the spectrum and latency of tumors, indicating the presence of modifiers of the outcome of *Trp53* deficiency.

We previously carried out a genome-wide scan for modifiers in thymic lymphomas that were induced by γ radiation in backcross mice and a consomic strain, also called a chromosome substitution strain, of the *Trp53*$^{+/-}$ genotype (*14*). As a result, a modifier designated as *Mp53D2* was assigned near *D19Mit90* on mouse chromosome 19. A peculiar feature of the *Mp53D2* locus is that the gene affects the development of thymic lymphomas only after irradiation in mice heterozygous for the *Trp53*-knockout allele. The incidence of lymphomas in irradiated *Trp53* wild-type mice was not affected by this locus. This genetic interaction

[1] Address for correspondence: Department of Molecular Genetics, Graduate School of Medical and Dental Sciences, Niigata University, Asahimachi 1-757, Niigata 951-812, Japan; e-mail: rykomina@med.niigata-u.ac.jp.

suggested that *Mp53D2* may target the Trp53-dependent signaling pathway. It is also possible, however, that the target is other Trp53-independent radiation-induced signaling pathways, through the Trp53-dependent and Trp53-independent pathways being interactive in determining the cell fate leading to lymphomagenesis. If the latter is the case, *Mp53D2* may not affect the development of thymic lymphomas in unirradiated *Trp53*-null mice.

To further dissect the process of lymphoma development with and without a functional *Trp53* gene, we produced *Trp53*$^{-/-}$ mice consomic for chromosome 19 and analyzed the development of thymic lymphomas. We also analyzed and compared the frequency of allelic loss between the radiation-induced lymphomas in *Trp53*$^{+/-}$ mice and the spontaneously developing thymic lymphomas in *Trp53*$^{-/-}$ mice, since allelic losses can be a consequence caused directly by γ radiation. These analyses revealed such interesting features as a lack of the effect of *Mp53D2* on the spontaneously development of thymic lymphomas and no requirement for the allelic loss at *Ikaros*. Furthermore, a region on chromosome 19 is suggested as harboring a novel tumor suppressor gene.

MATERIALS AND METHODS

Mice and Lymphoma Induction

We previously generated a consomic strain of BALB/c (C) background harboring chromosome 19 that was derived from the MSM (M) strain. Consomic strains are also called chromosome substitution strains (*15*). The female mice were mated with male BALB/c mice of *Trp53*-null genotype, and the *Trp53*$^{+/-}$ heterozygous mice were chosen by *Trp53* genotyping (*16*). Those mice were then crossed with *Trp53*$^{+/-}$ MSM mice. A total of 66 *Trp53*$^{-/-}$ mice of (BALB/c × MSM)F_1 background except for the chromosome 19 were followed up to 250 days after birth. Thymic lymphoma was diagnosed by observation of labored breathing and palpable induration of a thymic tumor. Existence of tumors was confirmed upon autopsy of the mice. Fifty-four of the 66 mice studied developed thymic lymphomas and seven developed other cancers such as skin tumors, some of which were examined histologically. The remaining five died of unknown causes. All animal experiments complied with the guidelines of the ethics committee for animal experimentation of Niigata University (written in Japanese).

DNA Isolation and Genotyping

Isolation of genomic DNA from brain and from thymic lymphomas was carried out by standard protocols. Genotyping of mice and allelic loss (LOH) analysis of spontaneously developing lymphomas were carried out with polymerase chain reaction (PCR) using microsatellite markers as described (*14*). Separation of PCR products was performed by 8% polyacrylamide gel electrophoresis. The γ-ray-induced thymic lymphomas analyzed in this study were those previously obtained in our laboratory (*14*). They developed in *Trp53*$^{+/-}$ heterozygous mice of both sexes that were subjected to γ irradiation with 2.5 Gy four times at weekly intervals, starting at the age of 4 weeks.

Statistics

χ^2 and P values for association of markers with the development of lymphomas were obtained by a χ^2 test and Mantel-Cox test with StatView-J 5.0 software. Evaluation of linkage followed the criteria of Lander and Kruglyak (*17*). The statistical threshold of the consomic mouse data was corrected for multiple comparisons using the formula, $\mu(T) = [C + 2\rho GT^2]\ \alpha(T)$; C (number of chromosomes) = 1, ρ (to account for corrected results among linked loci: for backcross with 1 *df*) = 1, G (genome size in morgans) = 0.47, T (for the χ^2 statistic with 1 *df*) = 3.84, and $\mu(T) = 0.05$. To achieve a false positive rate of 5% or less in the analysis of markers on the congenic region, we used a threshold of $P = 0.0034$.

RESULTS

The consomic mice of BALB/c (C) background used harbored a chromosome 19 derived from the MSM (M) strain. These mice were mated with BALB/c mice of the *Trp53*$^{-/-}$ genotype, and the offspring were then crossed with MSM mice of the *Trp53*$^{+/-}$ genotype. About one-fourth of the offspring obtained were of the *Trp53*$^{-/-}$ genotype. A total of 66 *Trp53*$^{-/-}$ mice were followed up to 250 days after birth. Most of the mice (54 mice) developed thymic lymphomas. Seven mice developed other cancers such as skin tumors. The remaining five died of unknown causes, and so these mice were excluded from this study. Genotyping with 11 markers on a region of chromosome 19 harboring the modifier *Mp53D2* (*D19Mit132* to *D19Mit103* in Table 1) revealed that 18 mice inherited the whole BALB/c chromosome from the heterozygous consomic mice and 15 the whole MSM chromosome, and 21 mice had chromosomes with recombinations at various regions.

Mice were divided into two groups, C/M and M/M genotypes, at the 11marker loci on chromosome 19. The Mantel-Cox test was performed at each locus for association between genotypes and latencies of thymic lymphoma development. No association was observed for any locus, including the *D19Mit90* locus harboring *Mp53D2*. Figure 1A displays the cumulative lymphoma latencies of homozygotes and heterozygotes at *D19Mit90*. Figure 1B shows for comparison the latencies in γ-ray-induced thymic lymphomas developed in *Trp53*$^{+/-}$ mice obtained previously (*14*). Mice of the M/M genotype developed lymphomas earlier than those of the C/M genotype. Compilation of these results indicated that the presence of the BALB/c or MSM allele near the *D19Mit90* locus did not provide susceptibility to spontaneously developing thymic lymphomas in *Trp53*$^{-/-}$ mice, whereas this locus did affect the incidence in irradiated *Trp53*$^{+/-}$ mice.

Figure 1C and D shows the effect of the sex of the mice on the spontaneously developing thymic lymphomas and on the γ-ray-induced thymic lymphomas, respectively. The *Trp53*$^{-/-}$ mice showed a clear sex difference in the latency of development of the spontaneous lymphomas in that the latency was shorter for males than females ($P = 0.033$ in Mantel-Cox test). In contrast, the *Trp53*$^{+/-}$ mice exhibited no such difference for radiation-induced lymphomas ($P = 0.58$).

The existence on chromosome 19 of functional tumor suppressor genes was suggested previously (*18*). A recent study implicated the *Pten* gene on chromosome 19 in the development of thymic lymphomas (*19*), suggesting the possibility that the *Mp53D2* modifier locus may be related

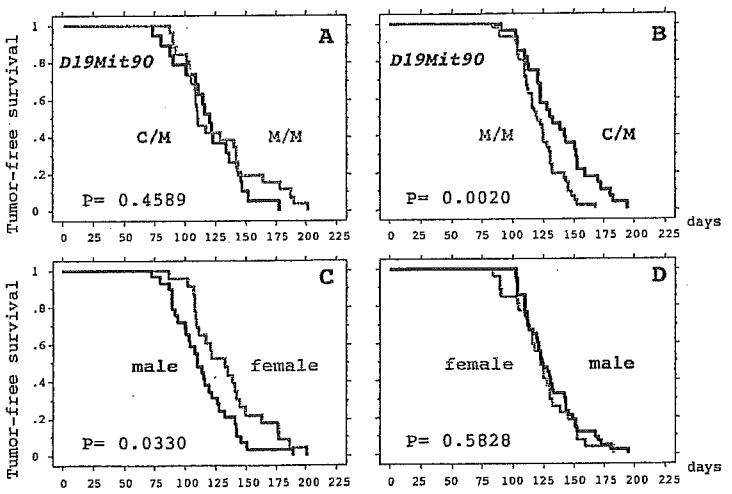

FIG. 1. Kaplan-Meier analysis of the cumulative frequency distributions of thymic lymphomas. Panel A: Distributions of spontaneously developed thymic lymphomas in progeny of *Trp53*$^{-/-}$ genotype. C/M, heterozygotes at *D19Mit90* and M/M, homozygotes at *D19Mit90*. Panel B: Distributions of γ-ray-induced thymic lymphomas in mice carrying a *Trp53*-deficient allele. C/M, heterozygotes at *D19Mit90* and M/M, homozygotes at *D19Mit90*. Panel C: Distributions of spontaneously developing thymic lymphomas in male and female mice of *Trp53*$^{-/-}$ genotype. Panel D: Distributions of γ-ray-induced thymic lymphomas in male and female mice of *Trp53*$^{+/-}$ genotype. *P* values for the difference between C/M and M/M genotypes in panels A and B and *P* values for the difference between male and female are calculated by Mantel-Cox test.

to or similar to the *Pten* gene. We tested this possibility by examining the allelic loss or loss of heterozygosity (LOH) in the thymic lymphomas. Allelic losses at the *Pten* and flanking marker loci are summarized in Fig. 2. Two LOH peaks were found, one at *Pten* and the other at *D19Mit39*, indicating the existence of a tumor suppressor gene in the vicinity of *D19Mit39* near but not at the *Pten* gene. We also examined LOH of the other 128 thymic lymphomas previously obtained in our laboratory (Table 1). The LOH frequency at *Pten* was 36% in *Trp53*$^{-/-}$ lymphomas and 30% (38/128) in the lymphomas developed in *Trp53*$^{+/-}$ mice.

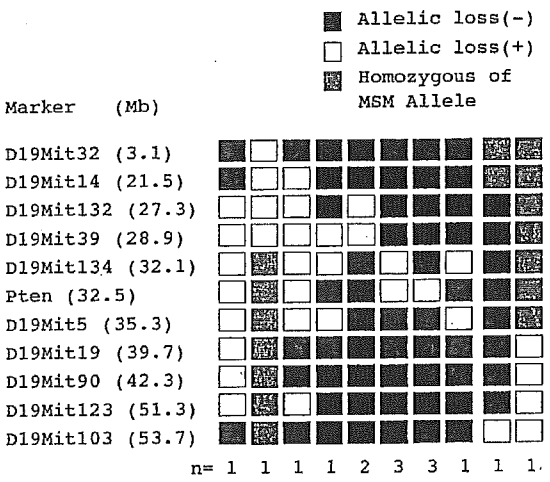

FIG. 2. Constitution of chromosome 19 in lymphomas. Open squares indicate loss of BALB/c or MSM allele, closed squares represent both BALB/c and MSM alleles retained, and gray squares show no information on LOH because the mice were homozygous. The number of lymphomas is listed at the bottom.

We have shown that three loci, *Ikaros, Rit1/Bcl11b* and *Tlsr7* on chromosomes 11, 12 and 16, respectively, displayed high frequencies of LOH in radiation-induced lymphomas (*16, 20–22*). Thus LOH frequencies of these loci were examined in the lymphomas that spontaneously developed (Fig. 3). The *Rit1/Bcl11b* and *Tlsr7* loci showed LOH at frequencies of 62 and 14%, respectively, comparable to those in the radiogenic thymic lymphomas of the previous studies (*16, 20–22*). On the other hand, the LOH frequency at *Ikaros* was 2% (1/50) in the spontaneously developing lymphomas; this was significantly lower than

TABLE 1
Distribution of Loci Showing LOH in Two Different Lymphomas

Marker (Mb)	Trp53$^{KO/KO}$ spontaneous	Trp53$^{KO/+}$ radiation-induced
D19Mit32 (3.1)	1/22 (5%)	ND
D19Mit14 (21.5)	2/23 (9%)	22/128 (17%)
D19Mit132 (27.3)	5/25 (23%)	27/128 (21%)
D19Mit39 (28.9)	6/25 (24%)	27/128 (21%)
D19Mit134 (32.1)	7/22 (32%)	29/128 (23%)
Pten (32.5)	8/22 (36%)	38/128 (30%)
D19Mit5 (35.3)	4/22 (18%)	23/128 (18%)
D19Mit19 (39.7)	2/22 (9%)	23/128 (18%)
D19Mit90 (42.3)	2/22 (9%)	23/128 (18%)
D19Mit123 (51.3)	3/21 (14%)	ND
D19Mit103 (53.7)	2/20 (10%)	ND

Notes. KO indicates a *Trp53*-deficient allele; + shows a wild-type allele of *Trp53*; ND, not determined.

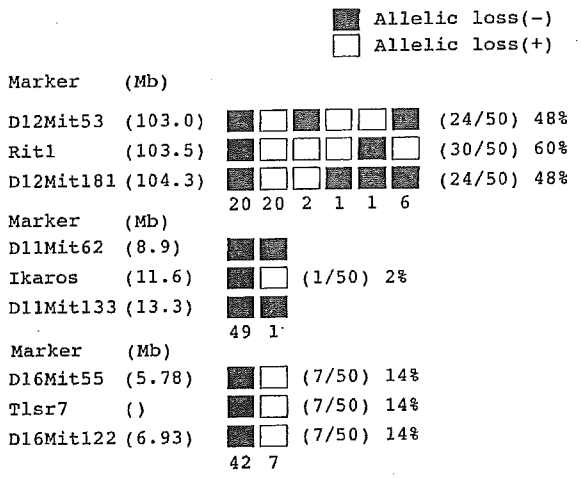

FIG. 3. Chromosomal constitutions of lymphomas near *Ikaros, Rit1/Bcl11b* and *Tlsr7*. The three loci used for analysis of allelic loss are indicated on the left. Open squares indicate loss of BALB/c or MSM allele and closed squares represent both BALB/c and MSM alleles retained. Gray squares show no information on LOH because the mice were homozygous. The number of lymphomas is shown at the bottom. The frequency of LOH is shown at the right.

the 78% (91/116) in the γ-ray-induced thymic lymphomas in *Trp53*$^{+/-}$ mice. Although this high frequency is partly due to the *Trp53* and *Ikaros* genes being located on the same chromosome 11, the high frequencies were also observed in *Trp53*$^{+/-}$ lymphomas retaining the *Trp53* wild-type allele (69%: 33/48) and in those of *Trp53*$^{+/+}$ mice (23%: 17/75) (*P* values less than 0.0001 and 0.0030, respectively) (*20*). The result suggests that *Ikaros* functions as a tumor suppressor in the development of the spontaneous thymic lymphomas only when the mice have a functional *Trp53* gene.

DISCUSSION

Genetic and environmental factors modulate the development of thymic lymphomas. We previously identified a *Trp53* modifier, designated as *Mp53D2*, on chromosome 19 by a genome scan of thymic lymphomas induced by γ radiation in *Trp53* heterozygous mice that did not affect the incidence or latency of lymphomas in *Trp53* wild-type mice (*14*). Most (70/85) of the lymphomas in *Trp53* heterozygotes lost the wild-type *Trp53* allele, indicating loss of Trp53 function (*14*). In the present study we examined the effect of *Mp53D2* on the development of thymic lymphomas that developed spontaneously without γ radiation. The two different *Mp53D2* genotypes studied did not differ in the latent period for lymphoma development in mice of the *Trp53*-null genotype. Compilation of these findings on lymphoma induction with three different genetic and environmental constitutions suggests that the action in lymphomagenesis of *Mp53D2* requires both *Trp53* deficiency as a genetic factor and γ radiation as an environmental factor, although effect of *Mp53D2* on the interaction between Trp53 function and radiation in mice is not clear. One possibility is that damages induced by γ radiation activate Trp53 proteins through Atm proteins and subsequently the Trp53 signaling pathway (*4, 23*), so that *Mp53D2* may play a role in this pathway. A database search was done for candidate genes that may be involved in this signaling pathway, but no obvious candidate was identified. Efforts are now being made to narrow the region containing the modifier by generating congenic strains harboring smaller MSM-derived regions and testing their influence on lymphoma development.

In contrast to the lack of an effect of *Mp53D2*, we observed sex differences in the latency of development of spontaneous thymic lymphomas but only when the mice were *Trp53*$^{-/-}$. The sex difference, which by itself is a well-known modifier of some kinds of tumor development (*24, 25*), was not seen in γ-ray-induced lymphomas, possibly because γ radiation obscured the sex difference.

Mapping of LOH regions localized two distinct loci on chromosome 19, one harboring *Pten* and another containing a possible novel tumor suppressor gene(s). *Pten* and *Trp53* are functionally related and both regulate cell proliferation and apoptosis (*26*). Pten proteins prevent Trp53 degradation mediated by Mdm2 and in turn Trp53 can bind to the *Pten* promoter and activate *Pten* transcriptionally (*27*), though this activation may have only a minor role in up-regulating *Pten* transcription (*28*). Interestingly, mutations in the *TP53* and *PTEN* genes are often mutually exclusive in human tumors (*29*), suggesting that loss of *PTEN* may reduce the selective pressure to lose *TP53* for the development of tumors. Frequent LOH at the *Pten* locus was reported in radiogenic mouse thymic lymphomas irrespective of *Trp53* genotype, indicating the involvement of *Pten* loss in lymphomagenesis (*18, 19*). The finding from the present study provides additional data to support this and suggests that loss of Trp53 function does not lead to reduction of the inactivation frequency of *Pten* in carcinogenesis despite predicted role of Trp53 in *Pten* regulation. Alternatively, Pten may have another Trp53-independent function.

Mapping analyses in our study identified two lymphomas with LOH near the *D19Mit39* locus not involving the *Pten* locus. LOH restricted to this same region was found in seven other cases among the γ-ray-induced thymic lymphomas (data not shown). These results indicate the presence of a novel tumor suppressor gene in the vicinity of the *D19Mit39* locus in addition to the already reported *Pten* gene. This may be consistent with the result of LOH mapping by Mao *et al.* (*19*). Further study is necessary to identify that gene and its role in tumor development.

LOH frequency was compared between the spontaneously developing lymphomas and γ-ray-induced thymic lymphomas (*16, 20–22*). Four loci on chromosomes 11, 12, 16 and 19 showed frequent LOH in the γ-ray-induced lymphomas, whereas only three of the four (all except *Ikaros* on chromosomes 11) exhibited frequent LOH in the spontaneously developing lymphomas. The frequency of LOH

for *Ikaros* was only 2%, indicating little or no involvement of the *Ikaros* tumor suppressor gene in lymphomas that developed spontaneously. It was reported (*30, 31*) that LOH and inactivation of *Ikaros* were also detected in chemical carcinogen-induced thymic lymphomas. On the other hand, *Rit1/Bcl11b* on chromosomes 12 showed 60–70% LOH in lymphomas of both spontaneous and radiogenic origin. This difference is difficult to explain. *Ikaros* and *Rit1/Bcl11b* both encode a family of zinc finger proteins and are essential for the development of the lymphoid system and subsequent T-cell development, respectively (*32–35*). *Ikaros*-knockout heterozygous mice exhibiting dominant negative effects on transcription have no fetal and adult lymphoid lineages. Overexpression of the dominant-negative Ikaros 6 isoform in cultured cells prevents apoptosis of the cells under certain conditions (*36–38*). These results suggest that lack of *Ikaros* activity leads to aberrant expansion of thymic clones due to escape from apoptosis and can eventually lead to T-cell neoplasia (32). On the other hand, *Rit1/Bcl11b*-knockout mice display selective defects in their αβ T-cell lineage, and their thymocytes undergo profound levels of apoptosis in newborns (*35*). The difference in cell death and proliferation between *Ikaros*- and *Rit1/Bcl11b*-deficient lymphatic cells might be a basis for the different LOH frequency. One possible explanation, as discussed above with *Pten,* is that loss of *Trp53* may reduce the selective pressure on lymphatic cells during lymphomagenesis to cause loss of *Ikaros*. If this is so, loss of *Ikaros* might contribute to the lymphoma development by preventing apoptosis through the Trp53 signaling pathway. Analysis of concomitant mutations in both *Ikaros* and *Trp53* in human malignancies should be informative, but no such study has been reported.

ACKNOWLEDGMENT

This work was supported by grants-in-aid of Second Term Comprehensive 10-year Strategy for Cancer Control from the Ministry of Health and Welfare of Japan.

Received: April 7, 2004; accepted: September 23, 2004

REFERENCES

1. J. B. Little, Radiation carcinogenesis. *Carcinogenesis* **21**, 397–404 (2000).
2. K. K. Khanna and S. P. Jackson, DNA double-strand breaks: Signaling, repair and the cancer connection. *Nat. Genet.* **27**, 247–254 (2001).
3. P. Fei and W. S. El-Deiry, P53 and radiation responses. *Oncogene* **22**, 5774–5783 (2003).
4. A. J. Giaccia and M. B. Kastan, The complexity of *p53* modulation emerging patterns from divergent signals. *Genes Dev.* **12**, 2973–2983 (1998).
5. T. Criswell, K. Leskov, S. Miyamoto, G. Luo and D. A. Boothman, Transcription factors activated in mammalian cells after clinically relevant doses of ionizing radiation. *Oncogene* **22**, 5813–5827 (2003).
6. P. Lichtlen and W. Schaffner, Putting its fingers on stressful situations: The heavy metal-regulatory transcription factor MTF-1. *Bioessays* **23**, 1010–1017 (2001).
7. D. Malkin, F. P. Li, L. C. Strong, J. F. Fraumeni, Jr., C. E. Nelson, D. H. Kim, J. Kassel, M. A. Gryka, F. Z. Bischoff and S. H. Friend, Germ line p53 mutations in a familial syndrome of breast cancer, sarcomas, and other neoplasms. *Science* **250**, 1233–1238 (1990).
8. M. S. Greenblatt, W. P. Bennent, M. Hollstein and C. C. Harris, Mutations in the p53 tumor suppressor gene: Clues to cancer etiology and molecular pathogenesis. *Cancer Res.* **54**, 4855–4878 (1994).
9. A. Balmain, J. Gray and B. Ponder, The genetics and genomics of cancer. *Nat. Genet.* **33**, 238–244 (2003).
10. B. A. J. Ponder, Cancer genetics. *Nature* **411**, 336–341 (2001).
11. R. T. Cormier, K. H. Hong, R. B. Halberg, T. L. Hawkins, P. Richardson, R. Mulherkar, W. F. Dove and E. S. Lander, Secretory phospholipase Pla2g2a confers resistance to intestinal tumorigenesis. *Nat. Genet.* **17**, 88–91 (1997).
12. L. A. Donehower, M. Harvey, B. L. Slagle, M. J. McArthur, C. A. Montgomery, J. S. Butel and A. Bradley, Mice deficient for p53 are developmentally normal but susceptible to spontaneous tumours. *Nature* **356**, 215–221 (1992).
13. C. J. Kemp, T. Wheldon and A. Balmain, p53-deficient mice are extremely susceptible to radiation-induced tumorigenesis. *Nat. Genet.* **8**, 66–69 (1994).
14. Y. Ochiai, Y. Tamura, Y. Saito, A. Matsuki, Y. Wakabayashi, Y. Aizawa, O. Niwa and R. Kominami, Mapping of genetic modifiers of thymic lymphoma development in *p53*-knockout mice. *Oncogene* **22**, 1098–1102 (2003).
15. JAX® Mice Strain Information. The Jackson Laboratory, Bar Harbor, ME, 2004. Available online at http://jaxmice.jax.org/info/index.html.
16. Y. Matsumoto, S. Kosugi, T. Shinbo, D. Chou, M. Ohashi, Y. Wakabayashi, K. Sakai, M. Okumoto, N. Mori and R. Kominami, Allelic loss analysis of gamma-ray-induced mouse thymic lymphomas: two candidate tumor suppressor gene loci on chromosomes 12 and 16. *Oncogene* **16**, 2747–2754 (1998).
17. E. Lander and L. Kruglyak, Genetic dissection of complex traits: Guidelines for interpreting and reporting linkage results. *Nat. Genet.* **11**, 241–247 (1995).
18. J. Santos, M. Herranz, M. Fernandez, C. Vaquero, P. Lopez and J. Fernandez-Piqueras, Evidence of a possible epigenetic inactivation mechanism operating on a region of mouse chromosome 19 in gamma-radiation-induced thymic lymphomas. *Oncogene* **20**, 2186–2189 (2001).
19. J. H. Mao, D. Wu, J. Perez-Losada, H. Nagase, R. DelRosario and A. Balmain, Genetic interactions between Pten and p53 in radiation-induced lymphoma development. *Oncogene* **22**, 8379–8385 (2003).
20. H. Okano, Y. Saito, T. Miyazawa, T. Shinbo, D. Chou, S. Kosugi, Y. Takahashi, S. Odani, O. Niwa and R. Kominami, Homozygous deletions and point mutations of the *Ikaros* gene in γ-ray-induced mouse thymic lymphomas. *Oncogene* **18**, 6677–6683 (1999).
21. A. Matsuki, H. Kosugi-Okano, Y. Ochiai, S. Kosugi, T. Miyazawa, Y. Wakabayashi, K. Hatakeyama, O. Niwa and R. Kominami, Allelic loss mapping and physical delineation of a region harboring a thymic lymphoma suppressor gene on mouse chromosome 16. *Biochem. Biophys. Res. Commun.* **282**, 16–20 (2001).
22. Y. Wakabayashi, J. Inoue, Y. Takahashi, A. Matsuki, H. Kosugi-Okano, T. Shinbo, Y. Mishima, O. Niwa and R. Kominami, Homozygous deletions and point mutations of the *Rit1/Bcl11b* gene in γ-ray induced mouse thymic lymphomas. *Biochem. Biophys. Res. Commun.* **301**, 598–603 (2003).
23. E. A. Slee, D. J. O'Connor and X. Lu, To die or not to die: How does p53 decide? *Oncogene* **23**, 2809–2818 (2004).
24. V. Di Majo, S. Rebessi, S. Pazzaglia, A. Saran and V. Covelli, Carcinogenesis in laboratory mice after low doses of ionizing radiation. *Radiat. Res.* **159**, 102–108 (2003).
25. J. M. Bugni, T. M. Poole and N. R. Drinkwater, The little mutation suppresses DEN-induced hepatocarcinogenesis in mice and abrogates genetic and hormonal modulation of susceptibility. *Carcinogenesis* **22**, 1853–1862 (2001).

26. D. J. Freeman, A. G. Li, G. Wei, H. H. Li, N. Kertesz, R. Lesche, A. D. Whale, H. Martinez-Diaz, N. Rozengurt and H. Wu, PTEN tumor suppressor regulates p53 protein levels and activity through phosphatase-dependent and -independent mechanisms. *Cancer Cell* **3**, 117–130 (2003).

27. V. Stambolic, D. MacPherson, D. Sas, Y. Lin, B. Snow, Y. Jang, S. Benchimol and T. W. Mak, Regulation of PTEN transcription by p53. *Mol. Cell* **8**, 317–325 (2001).

28. X. Sheng, D. Koul, J. L. Liu, T. J. Liu and W. K. Yung, Promoter analysis of tumor suppressor gene PTEN: Identification of minimum promoter region. *Biochem. Biophys. Res. Commun.* **292**, 422–426 (2002).

29. K. Kurose, K. Gilley, S. Matsumoto, P. H. Watson, X. P. Zhou and C. Eng, Frequent somatic mutations in PTEN and TP53 are mutually exclusive in the stroma of breast carcinomas. *Nat. Genet.* **32**, 355–357 (2002).

30. Y. Kodama, Y. Yoshikai, Y. Tamura, S. Wakana, R. Takagi, O. Niwa and R. Kominami, The *D5Mit7* locus on mouse chromosome 5 provides resistance to γ-ray induced but not N-methyl-N-nitrosourea-induced thymic lymphomas. *Cancinogenesis* **25**, 143–148 (2004).

31. A. Karlsson, P. Soderkvist and S. M. Zhuang, Point mutations and deletions in the znfn1a1/ikaros gene in chemically induced murine lymphomas. *Cancer Res.* **62**, 2650–2653 (2002).

32. S. Winandy, P. Wu and K. Georgopoulos, A dominant mutation in the *Ikaros* gene leads to rapid development of leukemia and lymphoma. *Cell* **83**, 189–299 (1995).

33. M. Cortes, E. Wong, J. Koipally and K. Georgopoulos, Control of lymphocyte development by the *Ikaros* gene family. *Curr. Opin. Immunol.* **11**, 167–171 (1999).

34. D. Liberg, S. T. Smale and M. Merkenschlager, Upstream of Ikaros. *Trends Immunol.* **24**, 567–570 (2003).

35. Y. Wakabayashi, H. Watanabe, J. Inoue, N. Takeda, J. Sakata, Y. Mishima, J. Hitomi, T. Yamamoto, M. Utsuyama and R. Kominami, *Bcl11b* is required for differentiation and survival of αβ T lymphocytes. *Nat. Immunol.* **4**, 533–539 (2003).

36. T. Yagi, S. Hibi, M. Takanashi, G. Kano, Y. Tabata, T. Imamura, T. Inaba, A. Morimoto, S. Todo and S. Imashuku, High frequency of Ikaros isoform 6 expression in acute myelomonocytic and monocytic leukemias: Implications for up-regulation of the antiapoptotic protein Bcl-xL in leukemogenesis. *Blood* **99**, 1350–1355 (2002).

37. N. Sezaki, F. Ishimaru, M. Takata, T. Tabayashi, K. Nakase, T. Kozuka, K. Fujii, H. Nakayama, T. Teshima and M. Tanimoto, Overexpression of the dominant-negative isoform of Ikaros confers resistance to dexamethasone-induced and anti-IgM-induced apoptosis. *Br. J. Haematol.* **121**, 165–169 (2003).

38. A. Ruiz, J. Jiang, H. Kempski and H. J. Brady, Overexpression of the Ikaros 6 isoform is restricted to t(4;11) acute lymphoblastic leukaemia in children and infants and has a role in B-cell survival. *Br. J. Haematol.* **125**, 31–37 (2004).

GASTROENTEROLOGY 2005;128:2089–2104

Long-term Extensive Expansion of Mouse Hepatic Stem/Progenitor Cells in a Novel Serum-Free Culture System

ATSUNORI TSUCHIYA,*† TOSHIO HEIKE,* HISANORI FUJINO,* MITSUTAKA SHIOTA,* KATSUTSUGU UMEDA,* MOMOKO YOSHIMOTO,* YASUNOBU MATSUDA,† TAKAFUMI ICHIDA,§ YUTAKA AOYAGI,† and TATSUTOSHI NAKAHATA*

*Department of Pediatrics, Graduate School of Medicine, Kyoto University, Kyoto; †Division of Gastroenterology and Hepatology, Graduate School of Medical and Dental Science, Niigata University, Niigata; and §Department of Gastroenterology, Juntendo University School of Medicine, Tagata-Gun, Japan

Background & Aims: The liver has high regenerative potential. We attempted to establish a novel culture system for extensive expansion of fetal mouse hepatic stem/progenitor cells and to characterize cultured cells. *Methods:* Hepatic spheroids collected from 6-day floating cultures were cultured on collagen-coated dishes in serum-free conditions in medium containing growth factors. Cultured cells were mainly characterized by immunocytochemistry and flow cytometry or transplanted into adult mice. *Results:* Approximately 400 expanding hepatic spheroids were generated from every 1×10^6 fetal liver cells. Subsequently, highly replicative colonies were subcultured with maintaining colony formation on collagen-coated dishes. These colonies consisted of small immature α-fetoprotein–positive cells and hepatocytic and cholangiocytic lineage-committed cells. The immature α-fetoprotein–positive cells could be expanded in a reproducible manner at least 5×10^5-fold (which involved at least 30 passages over >6 months) without losing differentiation potential. Flow cytometric analysis showed that all cultured cells expressed CD49f, but not CD34, Thy-1, c-kit, or CD45. Nearly 15% of the cells expressed Sca-1, and approximately 5%–20% of the cells were side population cells. Both sorted side population cells and Sca-1–positive cells (especially side population cells) produced a large number of α-fetoprotein–positive cells and lineage-committed cells. Expanded cells had bidirectional differentiation potential and improved serum albumin levels in mice with severe liver damage. *Conclusions:* Long-term extensive expansion of transplantable hepatic stem/progenitor cells was reproducibly achieved in a novel serum-free culture system. Moreover, this culture system yielded side population and Sca-1–positive cell populations that included hepatic stem/progenitor cells with differentiation and proliferation properties.

Liver transplantation is currently the ultimate therapy for many people with liver diseases, but the scarcity of donor organs and the risk of operative complications present serious drawbacks to this approach. An alternative approach may be to use hepatic stem cells that have dual differentiation potential as well as self-renewal and proliferation properties, because these cells will aid in the regeneration of damaged tissues.[1,2] However, this approach is impeded by the scarcity of donor cells. With regard to hepatic stem/progenitor cells, oval cells[3] and hepatocyte stem-like cells[4] from adult liver and hepatoblasts[5,6] and hepatocytic colony-forming units[7–9] from fetal liver have been identified as hepatic stem/progenitor cells. Recently, bone marrow cells,[10] cord blood cells,[11,12] and embryonic stem cells[13] are additional potential sources of hepatic stem/progenitor cells. However, a practical system that reproducibly and extensively expands hepatic stem/progenitor cells with differentiation capacities is yet to be established. Recently, analysis of mouse fetal liver by using fluorescence-activated cell sorter (FACS) and clonal culture systems, cells that fulfill the criteria for stem cells, were identified[7–9] in a $CD45^-$, $TER119^-$, $CD49f^{+/low}$, $c\text{-}kit^-$, $c\text{-}met^+$ fraction. However, it is not practical to use this approach because of the inherent complexities of purification and expansion difficulties. Furthermore, this procedure cannot be used with other species because of differences in cell-surface markers. In this study, we describe a novel and generally applicable system for extensive expansion of hepatic stem/pro-

Abbreviations used in this paper: AFP, α-fetoprotein; ALB, albumin; bFGF, basic fibroblast growth factor; BGP, biliary glycoprotein; CK, cytokeratin; CPSI, carbamoyl phosphate synthetase I; EGF, epidermal growth factor; FACS, fluorescence-activated cell sorter; FCS, fetal calf serum; FITC, fluorescein isothiocyanate; β-gal, β-galactosidase; HGF, hepatocyte growth factor; KSR, knockout serum replacement; MP, main population; OSM, Oncostatin M; PCR, polymerase chain reaction; SCC, small cell cluster; SP, side population; TAT, tyrosine amino transferase; TO, tryptophan-2, 3-dioxygenase.

0016-5085/05/$30.00
doi:10.1053/j.gastro.2005.03.030

genitor cells. We also show the growth, morphological, and cell marker characteristics of cultured cells.

In general, investigators use extracellular matrix–coated dishes for hepatic cell culture. However, in these culture methods, the rapid propagation of nonparenchymal cells and hematopoietic cells hampers proper amplification of hepatic stem/progenitor cells. Sphere formation has been used to select and amplify somatic stem cells from neural tissue,[14] mammary glands,[15] and skin.[16] We attempted to apply this sphere procedure in a new culture system. Although spheroid techniques have been used in hepatic cell research,[17,18] they were mainly used to maintain the functions of mature hepatocytes. Yasuchika et al[19] and Hoppo et al[20] recently reported that fetal liver cells formed spheroids upon culture on petri dishes for 12–16 hours in medium containing 10% fetal calf serum (FCS) and hepatocyte growth factor (HGF). However, the group cultured the cells for only 14 days and did not expand immature cells. To establish a culture system for extensive expansion of hepatic stem/progenitor cells, we examined several conditions, such as growth factors, culture time, and serum-free medium, for the formation of expanding spheroids. The resulting novel methods yielded more purified expanding spheroids containing hepatic stem/progenitor cells without the use of FACS than those produced by previous systems. Subsequent culturing of these spheroids by plating on collagen-coated dishes facilitated cultured cells to form expanding colonies. Furthermore, a new colony culture system that maintained cell–cell contact reproducibly induced the extensive expansion of immature and lineage-committed cells, which may be cell source candidates for cell therapies. Analysis of these cultured cells showed novel markers of hepatic stem/progenitor cells.

Materials and Methods

Animals

C57BL/6 mice obtained from SLC (Hamamatsu, Japan) and a pregnant C57BL/6 background β-galactosidase (β-gal) transgenic ROSA26 mouse obtained from Jackson Laboratories (Rochester, NY) for transplantation study were used. Mice were maintained according to the Animal Protection Guidelines of Kyoto University.

Dissociation of Fetal Liver Tissue

A pregnant C57BL/6 mouse at day 13.5 of gestation was killed and subjected to cesarean delivery. Fetal liver tissues were removed, dissected, placed in cold phosphate-buffered saline (PBS), dissociated by gentle mechanical pipetting, and collected by centrifugation at 500 rpm for 3 minutes.

Hepatic Spheroid Formation

Optimal growth conditions for spheroid formation were determined as described in the Results section. Finally, we used Dulbecco's modified Eagle medium/F12 (Sigma, St Louis, MO) with B27 (Gibco BRL, Grand Island, NY), ITS-X (Gibco), 10 mmol/L HEPES (Nakalai Tesque, Inc, Kyoto, Japan), antibiotics, 20 ng/mL epidermal growth factor (EGF; Sigma), 20 ng/mL basic fibroblast growth factor (bFGF; R&D Systems, Minneapolis, MN), and 20 ng/mL HGF (Sigma) as the standard medium. B27 is an auxiliary reagent that contains components such as bovine albumin (ALB), insulin, sodium selenite, and transferrin, as described in the article by Brewer et al.[21] This reagent is used to amplify stem/progenitor cells obtained from neural tissue,[14] mammary glands,[15] and skin.[16] Dissociated cells were plated on 6-well ultralow attachment plates (Corning, Corning, NY) at a density of 5×10^5 cells per milliliter in this standard medium. Standard medium was added at days 2 and 4. Hepatic spheroids bigger than 50 μm in diameter were counted at day 6.

Subculture on Collagen-Coated Dishes and Cryopreservation

Hepatic spheroids were collected at day 6 by centrifugation at 300 rpm for 2 minutes and plated on type I collagen–coated dishes (Becton Dickinson, San Jose, CA). After growing to subconfluency, cells were collected by using a solution of trypsin (final concentration of 0.2%; Gibco), Knockout Serum Replacement (KSR; final concentration of 20%; Gibco), and $CaCl_2$ (final concentration of 1 mmol/L; Nakalai Tesque) for 2 minutes. KSR, which is often used to maintain embryonic stem cells, is a supplement used in serum-free culture.[22] Collected cells were divided into 2 or 3 aliquots, replated on newly prepared collagen-coated dishes, and suspended in standard medium (the HGF concentration was reduced to 10 ng/mL after plating on collagen-coated dishes) every 6 days. Standard medium was changed every 3 days. For cryopreservation, we used Cell Banker (Nihonzenyaku, Fukushima, Japan). A flow diagram that describes our culture system is shown in Figure 1.

Differentiation Culture Conditions

To induce differentiation, cells were harvested from collagen-coated dishes and cultured at a density of 5×10^5 cells per milliliter for 6 days under 3 specific conditions: (1) matrigel-coated dishes (Becton Dickinson) with standard medium; (2) addition of 10 ng/mL Oncostatin M[23] (OSM; R&D Systems) to standard medium; and (3) medium containing FCS (Sigma) supplemented with various materials.[24]

Immunocytochemistry

Cells were washed in PBS, fixed with methanol (Wako, Osaka, Japan) at −20°C for 10 minutes, and incubated with primary antibodies overnight at 4°C and appropriate secondary antibodies for 30 minutes at room temperature. Antibodies were diluted to their optimal concentration in PBS containing

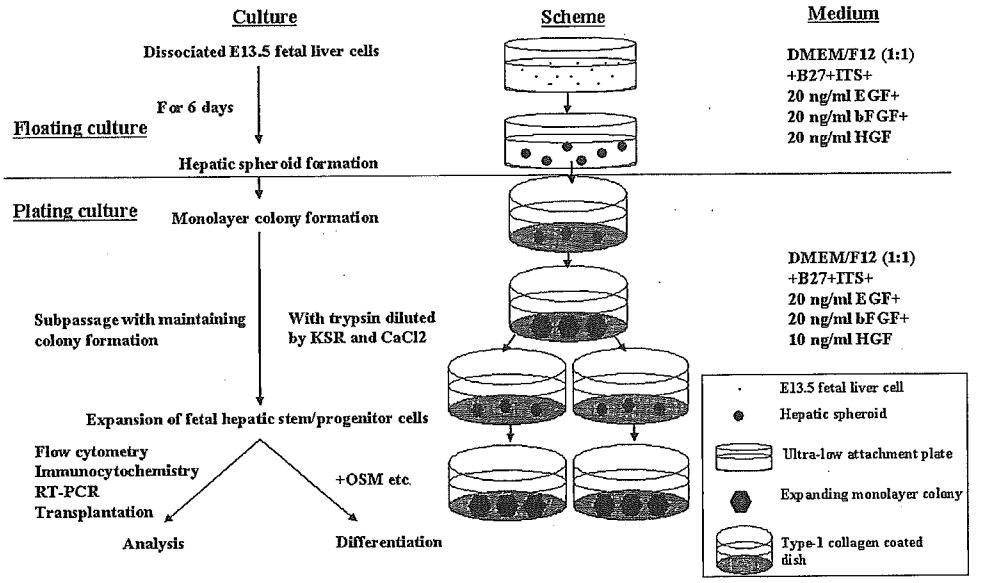

Figure 1. A flow diagram of our culture system. RT-PCR, reverse-transcription polymerase chain reaction; DMEM, Dulbecco's modified Eagle medium.

0.1% saponin. Primary antibodies used were goat anti-mouse ALB (Bethyl Laboratories, Inc, Montogomery, TX), rabbit anti-human α-fetoprotein (AFP; ICN Biochemicals, Costa Mesa, CA), mouse anti-cytokeratin (CK)7 (Progen, Heidelberg, Germany), rat anti-mouse E-cadherin (Takara Biochemicals, Otsu, Japan), goat anti-carbamoyl phosphate synthetase I (CPSI; Santa Cruz Biotechnology, Santa Cruz, CA), and rat anti-mouse Sca-1 (PharMingen, San Jose, CA). Secondary antibodies used were fluorescein isothiocyanate (FITC)-conjugated donkey anti-goat immunoglobulin (Ig)G, indocarbocyanine (Cy3)-conjugated donkey anti-goat IgG, FITC-conjugated donkey anti-rabbit IgG, Cy3-conjugated donkey anti-rabbit IgG, FITC-conjugated donkey anti-mouse IgG, and Cy3-conjugated donkey anti-rat IgG (Jackson ImmunoResearch Laboratories, Inc, West Grove, PA). Normal IgG of the species from which primary antibodies had been obtained served as primary antibodies in the negative controls. Nuclei were labeled with Hoechst 33342 (Molecular Probes, Eugene, OR). Periodic acid–Schiff staining was performed as described previously.[25]

Reverse-Transcription Polymerase Chain Reaction Analysis

Total RNA was prepared by using TRIzol (Invitrogen, Carlsbad, CA) and was reverse-transcribed by using a SuperScript first-strand synthesis system (Invitrogen). Complementary DNA was amplified by polymerase chain reaction (PCR) with the AmpliTaq Gold Kit (Applied Biosystems, Foster City, CA). PCR was performed by using primers for an immature cell marker, AFP; the hepatocyte-specific markers ALB, α_1-antitrypsin, glucose-6 phosphatase, tyrosine amino transferase (TAT),[20] and tryptophan-2, 3-dioxygenase (TO); the cholangiocyte-specific markers CK19 and biliary glycoprotein (BGP)[7]; and β-actin as an internal control. The following conditions were used for amplification: initial denaturation at 95°C for 9 minutes, followed by 25 (ALB and AFP), 30 (β-actin), or 35 (others) cycles of 94°C for 30 seconds, 56°C for 30 seconds, and 72°C for 30 seconds and a final extension step at 72°C for 10 minutes. PCR products were separated on 1.0% agarose gels.

Flow Cytometric Analysis and Hoechst 33342 Staining

We examined the cell-surface markers CD34,[26] Thy-1,[27] and c-kit[28] (known rat and human oval cell markers), CD49f[7] (the α_6-integrin subunit), CD45 (hematopoietic marker), and Sca-1. We additionally examined side population (SP) cells identified as having the ability to exclude dyes such as Hoechst because of their expression of transporter proteins. This effect was blocked by verapamil, a nonspecific inhibitor of membrane transport. Cells to be analyzed were harvested 6 to 10 weeks after plating with cell-recovery solution (Becton Dickinson) for 25 minutes. The resulting cells were incubated with anti-mouse CD16/32 antibodies[29] (PharMingen) for 15 minutes on ice to block nonspecific binding. Cells were then incubated with FITC-conjugated Sca-1, CD34, and Thy-1 antibodies; phycoerythrin (PE)-conjugated CD49f antibodies; and allophycocyanin (APC)-conjugated c-kit and CD45 antibodies (PharMingen) for 30 minutes on ice. FITC-conjugated rat IgG2a antibodies, phycoerythrin-conjugated rat IgG2a antibodies, and allophycocyanin-conjugated rat IgG2b antibodies (PharMingen) were used as isotype controls. Dead cells were excluded by propidium iodide (PI) gating. For the Hoechst staining, the dissociated cells (1×10^6/mL) were suspended in medium to which Hoechst 33342 was added (final concentration of 5 μg/mL) and incubated at 37°C for 90 minutes. In the control reactions, verapamil (Sigma) was added to a final concentration of 50 μg/mL. After washing, cells were analyzed with FACSCaliber and BD LSR (Lite Science Research) or sorted by using a FACSVantage with the CellQuest program (Becton Dickinson). To identify when CD45-negative Sca-1–

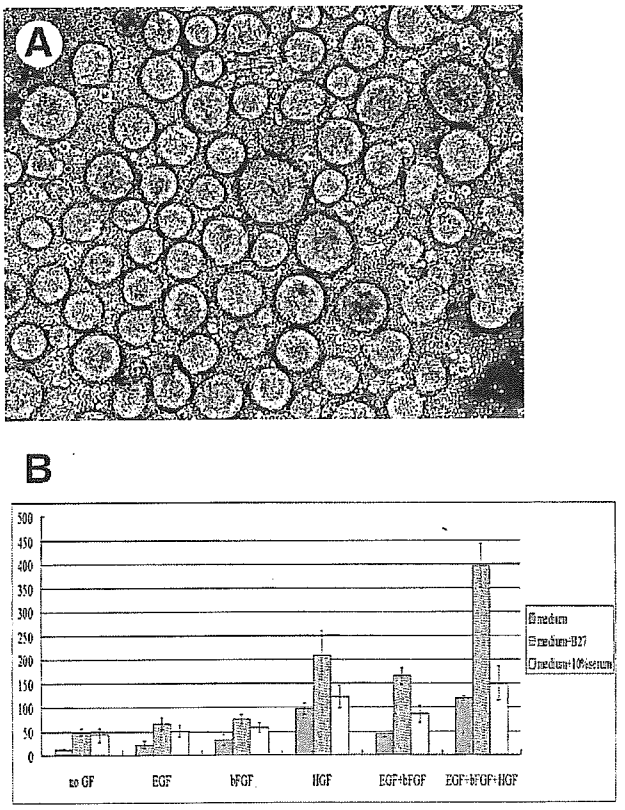

Figure 2. Hepatic spheroid formation at day 6 and investigation of optimal growth conditions. (*A*) Hepatic spheroids were obtained from floating cultures (original magnification, 100 ×). (*B*) The level of spheroid (>50 μm in diameter) formation at day 6 was highest in medium supplemented with B27, EGF, bFGF, and HGF.

positive cells and SP cells appeared, cultured cells were analyzed with FACSCaliber at days 0, 9, 15, 21, 27, 33, 39, and 45. To investigate which cell population in cultured cells actually proliferated, cultured cells were fractionated by using FACSVantage into 4 subpopulations: (1) SP, Sca-1–negative cells; (2) SP, Sca-1–positive cells; (3) main population (MP), Sca-1–positive cells; and (4) MP, Sca-1–negative cells. Fractionated cells were stained with anti-AFP antibodies or single cells were cultured in individual wells of 96-well collagen-coated dishes. At day 14 after sorting, large colonies occupying more than 70% of wells were counted. To examine the bidirectional differentiation potential of cultured cells, 10 large colonies of each subpopulation were cultured for 2 months and immunostained with anti-AFP, -ALB, and -CK7 antibodies. The frequency of SP cells and Sca-1–positive cells in these colonies was analyzed sequentially by using FACSCaliber and BD LSR.

Transplantation and Immunohistochemistry

For transplantation, β-gal transgenic ROSA26 fetal liver cells at day 13.5 of gestation were expanded for 2 months as described previously. Liver damage was induced in recipient mice (n = 5; 8 weeks old; male) before transplantation by injecting 2 mL/kg carbon tetrachloride dissolved in olive oil 6 times at 4-day intervals. Then, 2 days after the last carbon tetrachloride administration, we injected 1×10^6 expanded cells in 0.1 mL of standard medium with a 30-gauge needle into the left lateral lobe of damaged livers. For immunohistochemistry, 30 days later, recipient livers were harvested and were fixed with 4% paraformaldehyde overnight at 4°C. X-gal (Nakalai Tesque) staining was performed as described previously,[30] and the livers were then embedded in OCT compound and sectioned. Cryostat sections were incubated with horseradish peroxidase–conjugated goat anti-mouse ALB (Bethyl Laboratories) and mouse anti-CK19 (Dako, Kyoto, Japan) and then stained by using DAB Substrate Kit, M.O.M Kit, and Vectastain ABC Kit (Vector Laboratories, Burlingame, CA). To assess whether expanded cells would improve liver functions in mice damaged by carbon tetrachloride treatment as described previously, half of the treated mice (n = 7) received 3×10^6 expanded cells in their spleen, and the other half (n = 7) received medium only (sham transplantation). Mice that survived beyond 24 hours were examined. Blood samples were collected at days 0, 6, 12, and 18 after transplantation and were tested for prothrombin time, serum total bilirubin, ALB, and cholinesterase (FALCO Biosystems, Kyoto, Japan).

Statistical Analysis

Data are presented as means ± SD. Student *t* tests were used to determine statistical significance.

Results

Expanding Spheroid Formation by Using a Floating Culture System

We initially attempted to generate hepatic spheroids by using a floating culture system. After evaluating 3 different culture conditions, including (1) no supplement, (2) medium containing B27, and (3) medium containing 10% FCS, the contributions of growth factors (EGF, bFGF, and HGF) were examined. High levels of spheroid formation were observed under condition 2 compared with conditions 1 and 3. Next, we estimated the effects of the growth factors—EGF, bFGF, and HGF—under B27-supplemented conditions. EGF, bFGF, and HGF formed spheroids 1.2-fold, 1.2-fold, and 4-fold more efficiently than no growth factor, respectively. Thus, HGF was the most effective individual growth factor in inducing spheroid formation. Surprisingly, a combination of EGF and bFGF induced the formation of 3-fold more spheroids, and a combination of EGF, bFGF, and HGF led to 8-fold more spheroids than no growth factor (Figure 2). Accordingly, medium supplemented with B27, EGF, bFGF, and HGF was used as standard medium in all subsequent experiments. After dissociation of fetal liver tissue into single cells, culture was continued in standard medium, and this led to reaggregation (similar to a bunch of grapes[5]) within

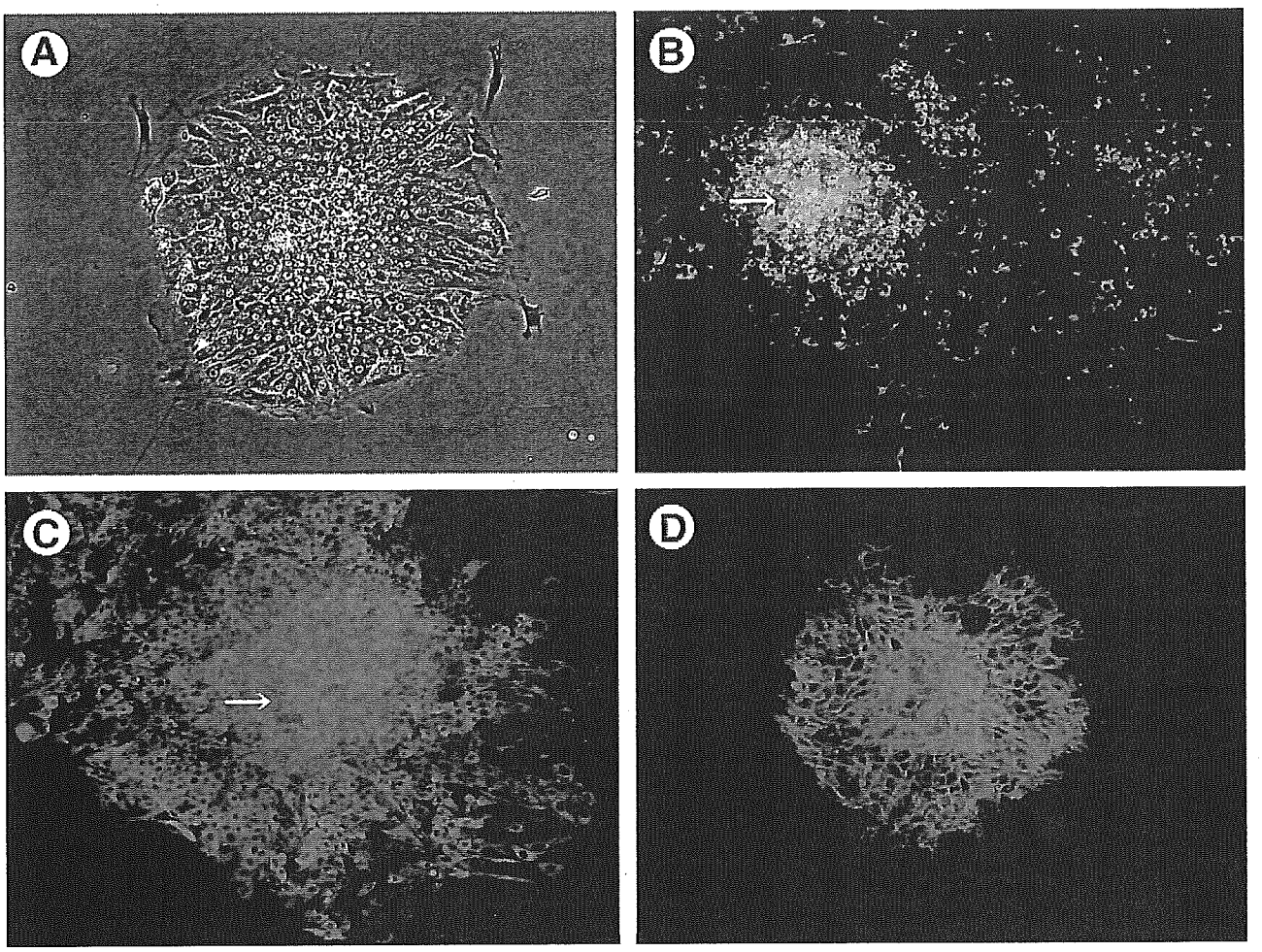

Figure 3. Colony formation after plating on collagen and immunocytochemical profiles. (*A*) Monolayer colonies were formed from spheroids at day 2 after plating. In these colonies, (*B*) ALB-positive (*green*) and (*C*) AFP-positive (*red*) cells were observed in the center, and (*B*) CK7-positive (*red*) cells were detected in the periphery. (*D*) Almost all cells expressed E-cadherin (*red*). *Arrows* indicate the center of the colonies (original magnification, 100×).

24 hours. Over the next 2–3 days, more than 50% of cells formed spheroids that displayed a ball-like shape (20–100 μm in diameter). The spheroids increased to a diameter of approximately 50–250 μm, comprising approximately 20–150 cells, and reached a plateau level within 6 days. On average, from 1×10^6 fetal liver cells cultured in standard medium, approximately 400 spheroids were formed.

Culture of Hepatic Stem/Progenitor Cells on Collagen-Coated Dishes

We attempted to dissociate spheroids by mechanical pipetting or enzymatic digestion while maintaining their viability and ability to repeatedly form new spheroids for expansion. However, this approach was unsuccessful. Next, we plated spheroids on type I collagen–coated dishes in standard medium at day 6. Within 48 hours, more than 90% of spheroids formed monolayer colonies (Figure 3*A*) and then expanded. Immunocytochemistry analysis of these colonies showed cells that expressed ALB (hepatocytic lineage) and AFP (immature cells) in the center and CK7-positive (cholangiocytic lineage) cells at the periphery (Figure 3*B* and *C*). Almost all cells expressed E-cadherin (Figure 3*D*), thus indicating that these colonies consist of epithelial cells.

Analysis of Long-term Cell Culture

We next attempted to expand hepatic stem/progenitor cells extensively. Although we generally use trypsin/ethylenediaminetetraacetic acid (EDTA) for collecting adhesive cells, it is difficult to maintain viable fetal liver cells. To overcome this problem, trypsin was diluted in KSR, and $CaCl_2$ was added as described in Materials and Methods. This stimulated detachment of colonies from the collagen-coated dish while allowing them to maintain cell–cell

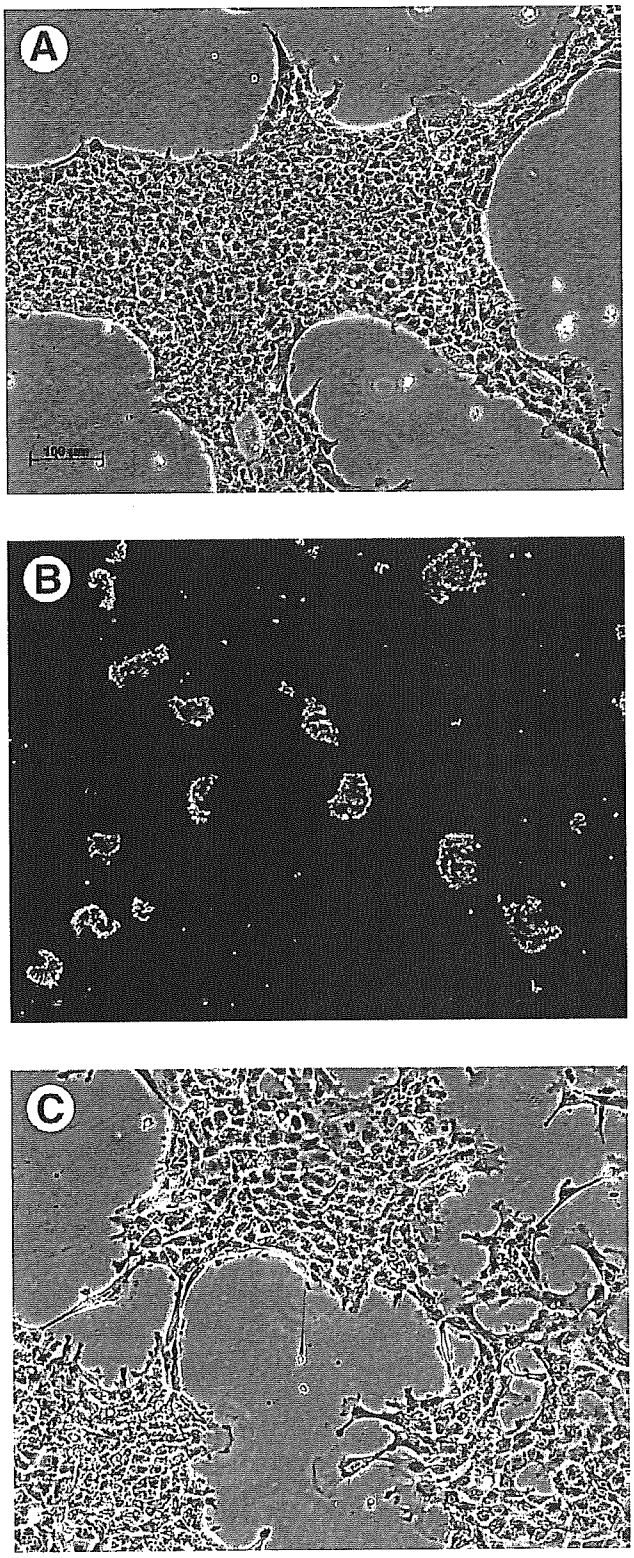

Figure 4. Time course of cell collection. The pictures depict cells (*A*) before passage, (*B*) during passage, and (*C*) after passage. (*B*) During passage, cell–cell contact was maintained (original magnifications: *A* and *C*, 100 ×; *B*, 40×).

contact. This technique preserved the viability of fetal liver cells (>80%) without loss of colony formation. Small colonies reformed larger colonies after plating. Thus, we could easily expand cells in this fashion (Figure 4). At day 21 after plating, cultured cells began to form larger colonies containing small cell clusters (SCCs; 10%–30% of total cells) in the center of the colonies (Figure 5*A* and *B*). SCCs comprised a large number of small cells, with a high nuclear/cytoplasmic ratio, that were singly or doubly positive for AFP and/or ALB (Figures 5*C* and 6*A*). These SCCs were surrounded by CK7-positive cells (Figure 6*B* and *C*). To examine whether SCCs have growth ability, we picked an SCC, placed it on collagen, and observed its growth. As shown in Figure 5*D–F*, SCCs had extensive growth potential. After the formation of SCCs, cultured cells consisted of E-cadherin–positive epithelial cells (Figure 6*D*), and cell growth increased steadily by 2–3-fold in 6 days. These experiments were repeated 5 times and yielded reproducible results. Figure 6*E* depicts growth curves in 1 case. Extensive growth of both total cells and AFP-positive cells was observed. Our established cultured cells permitted subculturing for >6 months with a minimum of 30 passages. Over a 6-month period, AFP-positive immature cells expanded at least 5×10^5-fold. Thus, we have successfully established a novel culture system for the extensive expansion of hepatic stem/progenitor cells. Moreover, when we cryopreserved expanded cells by freezing in Cell Banker, we found that upon thawing they continued to expand vigorously.

Differentiation Potential of Cultured Cells

E13.5 liver expresses the genes for AFP, ALB, α_1-antitrypsin, CK19, and BGP. In our culture system, cells continued to express genes for AFP, ALB, α_1-antitrypsin, glucose-6 phosphatase, CK19, and BGP but did not express hepatocytic differentiation markers (TAT and TO) for 4 months (Figure 7*A*). Some cultured cells were strongly positive for glycogen or CPSI. For clinical application, the capacity to differentiate and mature is requisite. Accordingly, we induced differentiation by culturing cells on matrigel-coated dishes, adding OSM (a growth factor that induces differentiation of hepatocytes), and replacing with medium containing FCS, as described in Materials and Methods. TAT and TO expression was induced under all the conditions examined, as shown by reverse-transcription PCR. Upon the addition of OSM and FCS, small cells decreased to <10%, whereas that of large cells increased, with most of the latter staining for glycogen and CPSI (Figure 7*B* and *C*). Moreover, morphologically mature hepatocytes with bile canalicular-like structures between them were consistently observed under these culture conditions (Figure 7*D*).

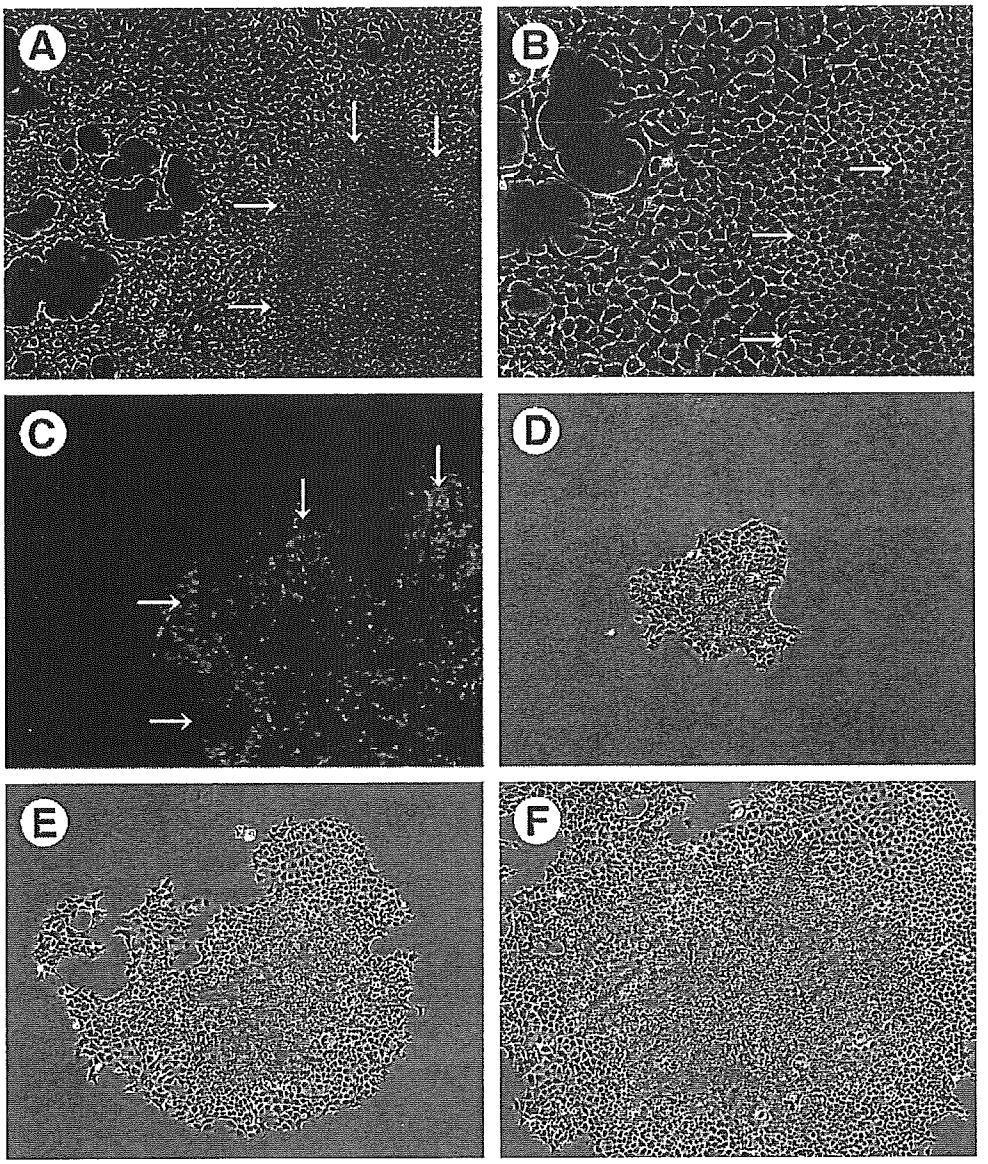

Figure 5. Colony formation at day 21 after plating on collagen. (*A* and *B*) Large colonies consisting of small cells (SCCs; *arrows*) surrounded by large cells were formed. Small cells had a high nuclear–cytoplasmic ratio. (*C–F*) SCCs contained immature small AFP-positive (*red*) cells and had extensive growth ability. (*D–F*) Sequential appearance of a replated SCC (*D*, day 1; *E*, day 2; *F*, day 3; original magnifications: *A* and *C–F*, 40×; *B*, 100×).

Analysis of Sca-1–Positive Cells and Side Population Characteristics of Long-term Cultured Cells

To characterize cells in long-term culture, we analyzed cell-surface markers and SP characteristics by flow cytometry. Markers for rat and human oval cells (CD34, Thy-1, and c-kit) or hematopoietic cells (CD45) were not detected. However, almost all cells expressed CD49f. In short, cultured cells are in a $CD34^-$, $Thy\text{-}1^-$, $c\text{-}kit^-$, $CD45^-$, $CD49f^+$ fraction. In this fraction, nearly 15% of the cells expressed Sca-1 (Figure 8), and approximately 5%–20% of the cells contained SP cells (Figure 9*B* and *C*). We did not detect CD45-negative, Sca-1–positive cells or SP cells during the early stages of culture, but from day 15 and 21, respectively, they became detectable, and their numbers began to increase. Their frequency reached a plateau at day 33 and was maintained thereafter (Figure 9*A*). Next, we compared Sca-1–positive cells, SP cells, and AFP-positive immature cells with respect to size and distribution. Immunocytochemistry results disclosed the presence of small AFP-positive cells in the center of the colonies and larger Sca-1–positive cells at the periphery of small cells (Figure 10*A* and *B*). Approximately 1%–3% of Sca-1–positive cells were overlapped with AFP-positive cells. Flow cytometric analysis indicated that the overall size of SP cells is smaller than that of Sca-1–positive cells (data not shown). SP cells were identified as predominantly small cells (more than 50%; Figure 9*D*). Approximately 10% of SP cells overlapped with Sca-1–positive cells (Figure

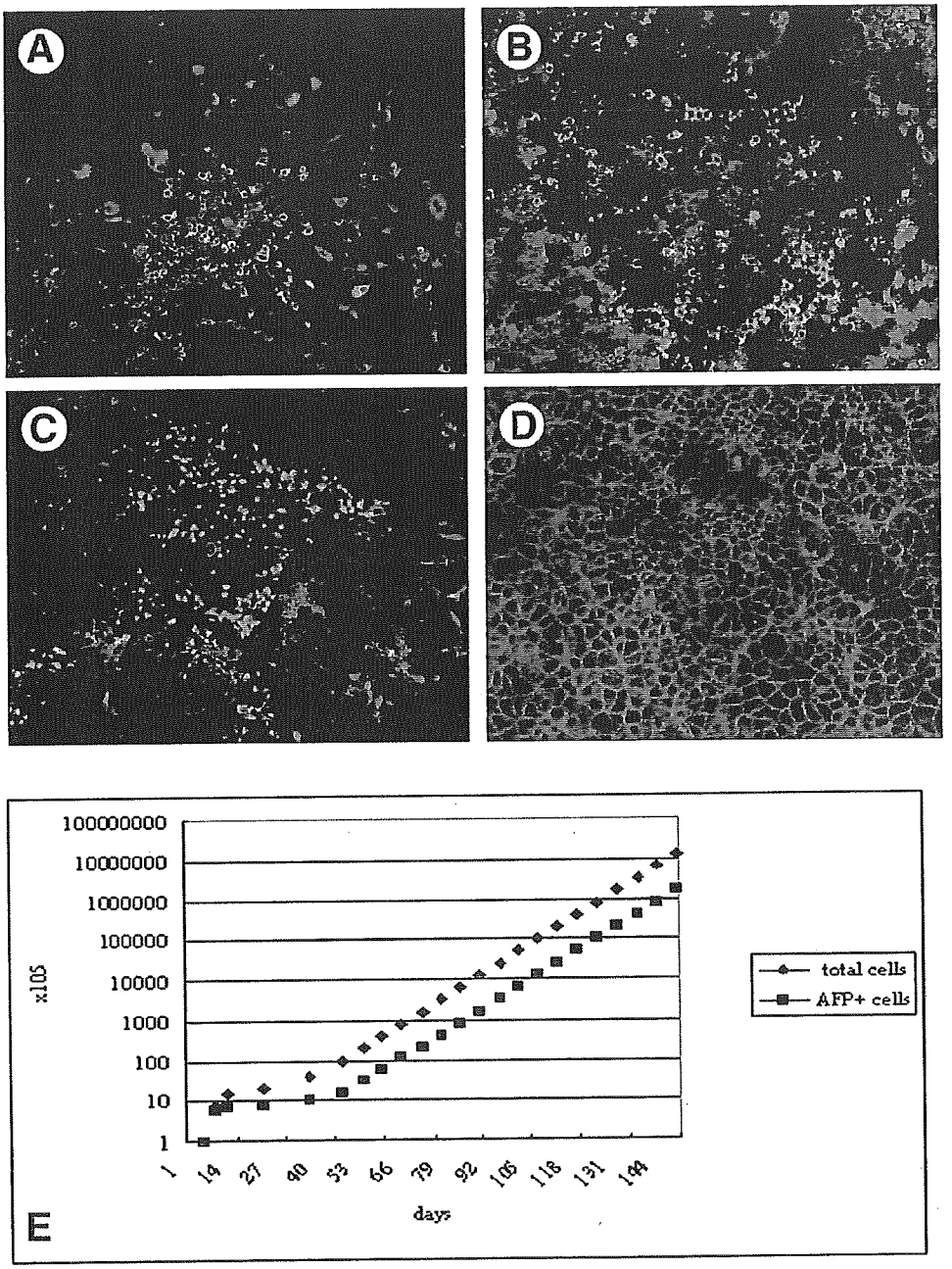

Figure 6. Immunocytochemistry of long-term cultured cells at day 60. Merged views of (*A*) ALB-positive (*green*), AFP-positive (*red*), and double-positive (*yellow*) cells; (*B*) AFP-positive (*green*) and CK7-positive (*red*) cells; and (*C*) ALB-positive (*green*) and CK7-positive (*red*) cells are shown. (*D*) Cultured cells were strongly or weakly positive for E-cadherin. (*E*) The growth time courses of total cells and AFP-positive cells are shown for 1 representative example. Each point corresponds to a passage point (original magnification, *A–D*: 100×).

9*E*). Our results collectively indicate that the overall size of Sca-1–positive cells is larger than that of AFP-positive cells and SP cells. To investigate which cell population actually contains AFP-positive cells or has the ability to form large colonies, cultured cells were fractionated into 4 subpopulations: (1) SP, Sca-1–negative cells; (2) SP, Sca-1–positive cells; (3) MP, Sca-1–positive cells; and (4) MP, Sca-1–negative cells. The cells in groups 1 and 2 had more AFP-positive cells than those in groups 3 and 4: the frequency of AFP-positive cells was (1) 72.0% ± 3.6%, (2) 70.7% ± 4.2%, (3) 2.3% ± 1.5%, and (4) 0.6% ± 0.6% (Figure 10*C* and *D*). Moreover, single-cell culture of each subpopulation showed that the cells in groups 1 and 2 had a greater ability to form large colonies than those in groups 3 and 4 (Figure 10*G*). Finally, 10 large colonies derived from a single cell of each subpopulation were followed up, immunostained, or analyzed by flow cytometry. All large colonies grew efficiently with increasing the number of SP cells and Sca-1–positive cells (data not shown) and contained AFP-, ALB-, and CK7-positive cells (Figure 10*E* and *F*).

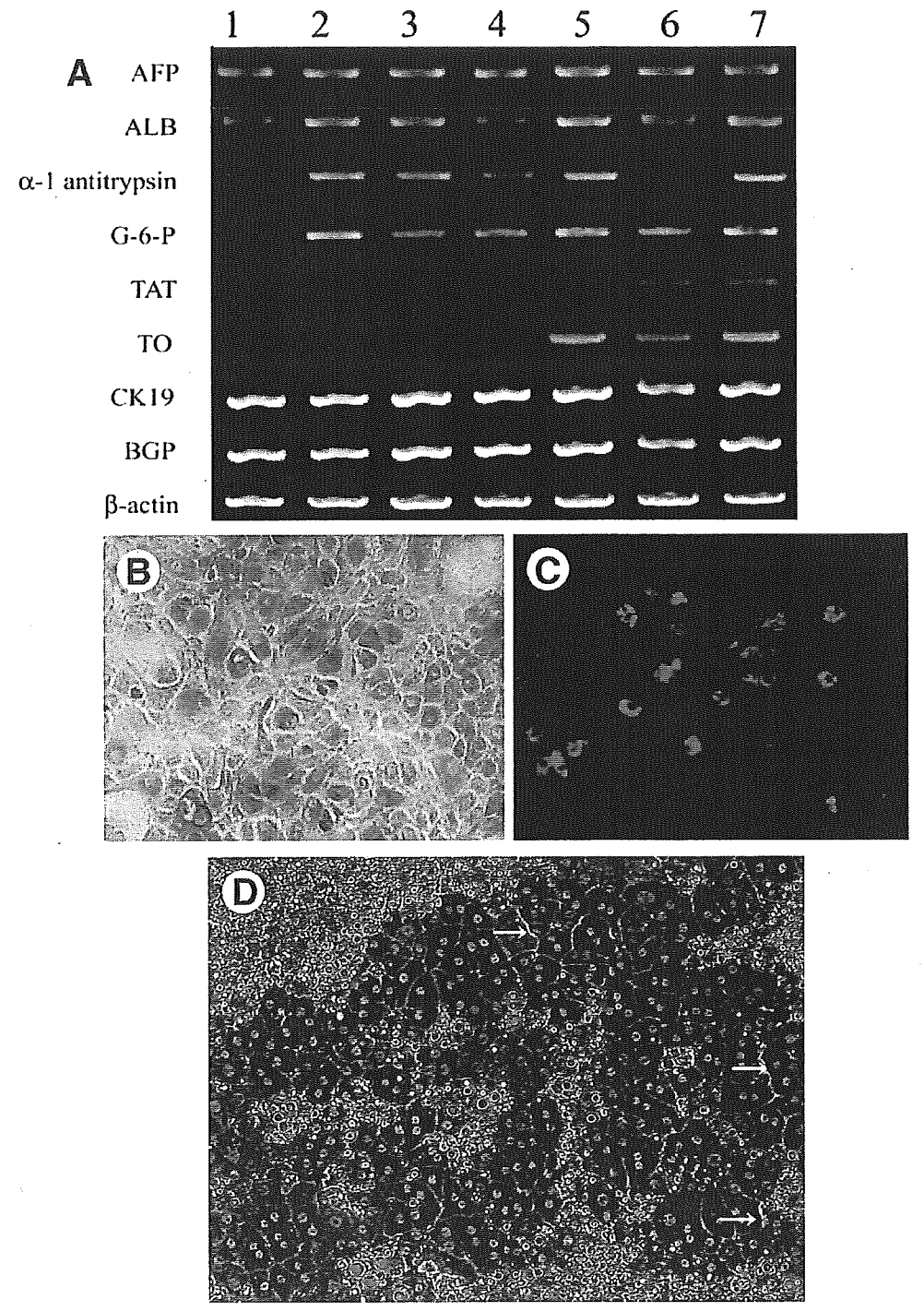

Figure 7. Reverse-transcription PCR analysis and cytochemistry of cells cultured in serum-free and differentiation conditions. (*A*) The following lanes were analyzed: E13.5 fetal liver (lane 1); cultured cells at day 14 (lane 2), day 75 (lane 3), and day 120 (lane 4); culture on matrigel for 6 days at day 60 (lane 5); culture to which OSM was added for 6 days at day 60 (lane 6); and culture with medium containing FCS for 6 days at day 60 (lane 7). Samples in lanes 1–4 did not express TAT and TO, whereas those in lanes 5–7 expressed TAT and TO. After the addition of OSM, large cells were strongly stained with (*B*) periodic acid–Schiff and (*C*) CPSI (*red*). (*D*) Morphologically mature hepatocytes were observed in these differentiation conditions. *Arrows* indicate bile canalicular-like structures. G-6-P, glucose-6 phosphatase (original magnification, *B–D*: 200×).

Transplantation of Cultured Cells

To show the ability of long-term cultured cells to populate damaged adult livers, we generated long-term fetal hepatic stem/progenitor cell cultures from β-gal transgenic ROSA26 mouse fetal livers. These cells were transplanted into adult livers that had been damaged by carbon tetrachloride treatment. At day 30 after transplantation, β-gal–positive areas were diffusely detectable in all the transplanted livers (Figure 11*A*). Moreover, immunohistochemistry for ALB or CK19 showed the presence in the transplanted adult livers of ALB and β-gal double-positive cells (hepatocytic lineage: Figure 11*B* and *C*) and of CK19 and β-gal double-positive cells with bile duct–like struc-

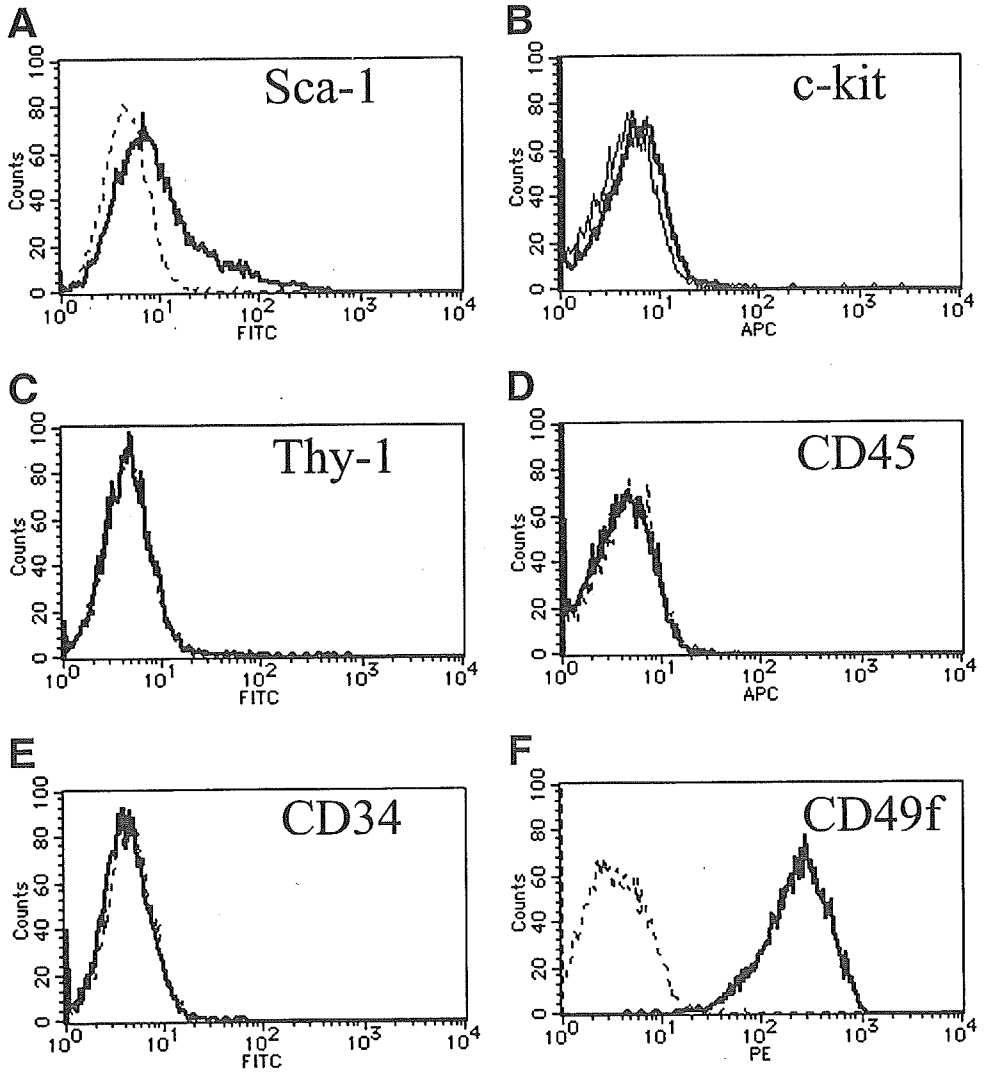

Figure 8. Flow cytometric analysis of cultured cells. The histograms represent expression of the antigens (*A*) Sca-1, (*B*) c-kit, (*C*) Thy-1, (*D*) CD45, (*E*) CD34, and (*F*) CD49f. Plots display the isotype control staining profiles (*dashed lines*) vs specific antibody staining profiles (*solid lines*). APC, allophycocyanin; PE, phycoerythrin.

tures (cholangiocytic lineage: Figure 11*D* and *E*). To assess whether expanded cells would improve liver function in mice damaged by carbon tetrachloride treatment, half of the treated mice (n = 7) received 3 × 10^6 expanded cells into their spleens, whereas the other half (n = 7) received medium only (sham transplantation). There were no statistically significant differences in prothrombin time, serum total bilirubin, or cholinesterase levels (data not shown). However, as shown in Figure 11*F*, serum ALB levels in the cell transplantation group increased more rapidly than those in sham transplantation group. At day 12, serum ALB levels were significantly higher in the cell transplantation group ($P < .05$) than those in the sham transplantation group. These results indicate that although the functional benefit of these cells is limited in this model, they certainly have the potential to improve liver function.

Discussion

There are various reports in the literature of long-term culture of fetal hepatic stem/progenitor cells. However, most of these studies focus on the differentiation process.[25,31] With regard to the expansion of immature hepatic cells that maintain their differentiation potential, Suzuki et al[7–9] identified a fraction of $CD45^-$, $TER119^-$, $CD49f^{+/low}$, $c\text{-}kit^-$, $c\text{-}met^+$ cells obtained from mouse fetal liver as hepatic stem/progenitor cells by using FACS. However, their procedure had limitations due to inherent purification complexities and expansion difficulties. In addition, the group used medium with FCS and did not specifically investigate the presence of immature markers such as AFP and Sca-1 or SP. Recently, Lázaro et al[32] succeeded in culturing human fetal liver cells over the long term that maintained hepatocytic and cholangiocytic traits in serum-free medium supple-

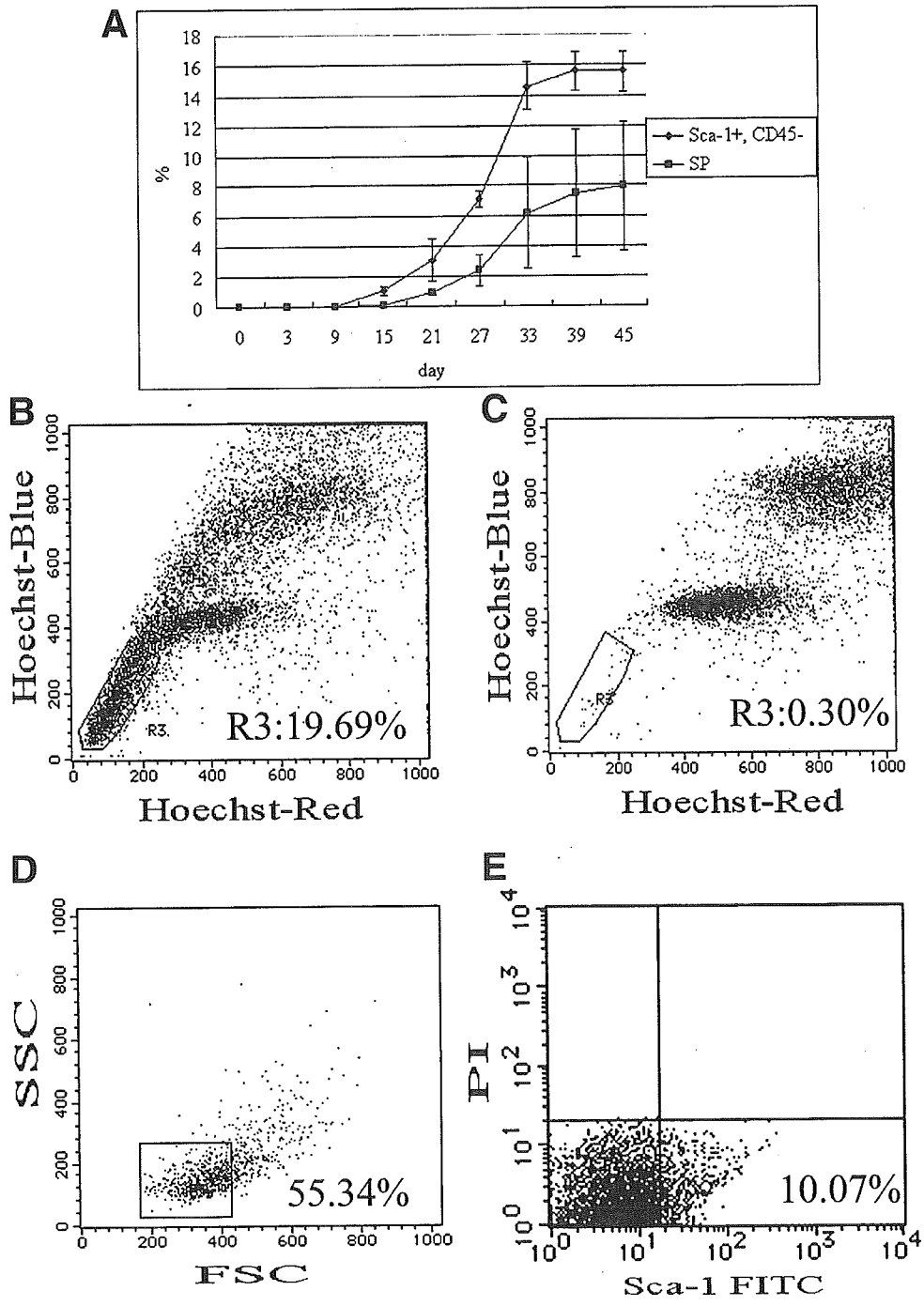

Figure 9. Flow cytometric analysis of SP cells and Sca-1–positive cells. (*A*) Analysis of the appearance of CD45-negative Sca-1–positive cells and SP cells is shown. They gradually increased and reached a plateau at day 33, after which their frequency was maintained. (*B*) A low Hoechst-staining population (SP cells) was identified in the fraction gated R3. (*C*) The Hoechst dye was blocked by verapamil in the fraction gated R3. (*D*) SP cells (R3) were predominantly small. (*E*) Approximately 10% of SP cells (R3) overlapped with Sca-1–positive cells. PI, propidium iodide; FSC, forward scatter; SSC, side scatter.

mented with EGF. However, although this group succeeded in subculturing fetal liver cells for 2 passages, they failed to expand immature hepatic cells for longer periods. Thus, we attempted to establish a novel culture system for extensive expansion of hepatic stem/progenitor cells.

Sphere formation has been used to select and amplify somatic stem cells in various tissues.[14–16] We modified this method to enrich hepatic stem/progenitor cells. From floating cultures grown for 6 days, we efficiently obtained approximately 400 enriched expanding spheroids per 1×10^6 cells in serum-free medium supplemented with B27, EGF, bFGF, and HGF.

Because we could not effectively continue to expand spheroids because of resistance to dissociation, we cultured spheroids on collagen-coated dishes and success-

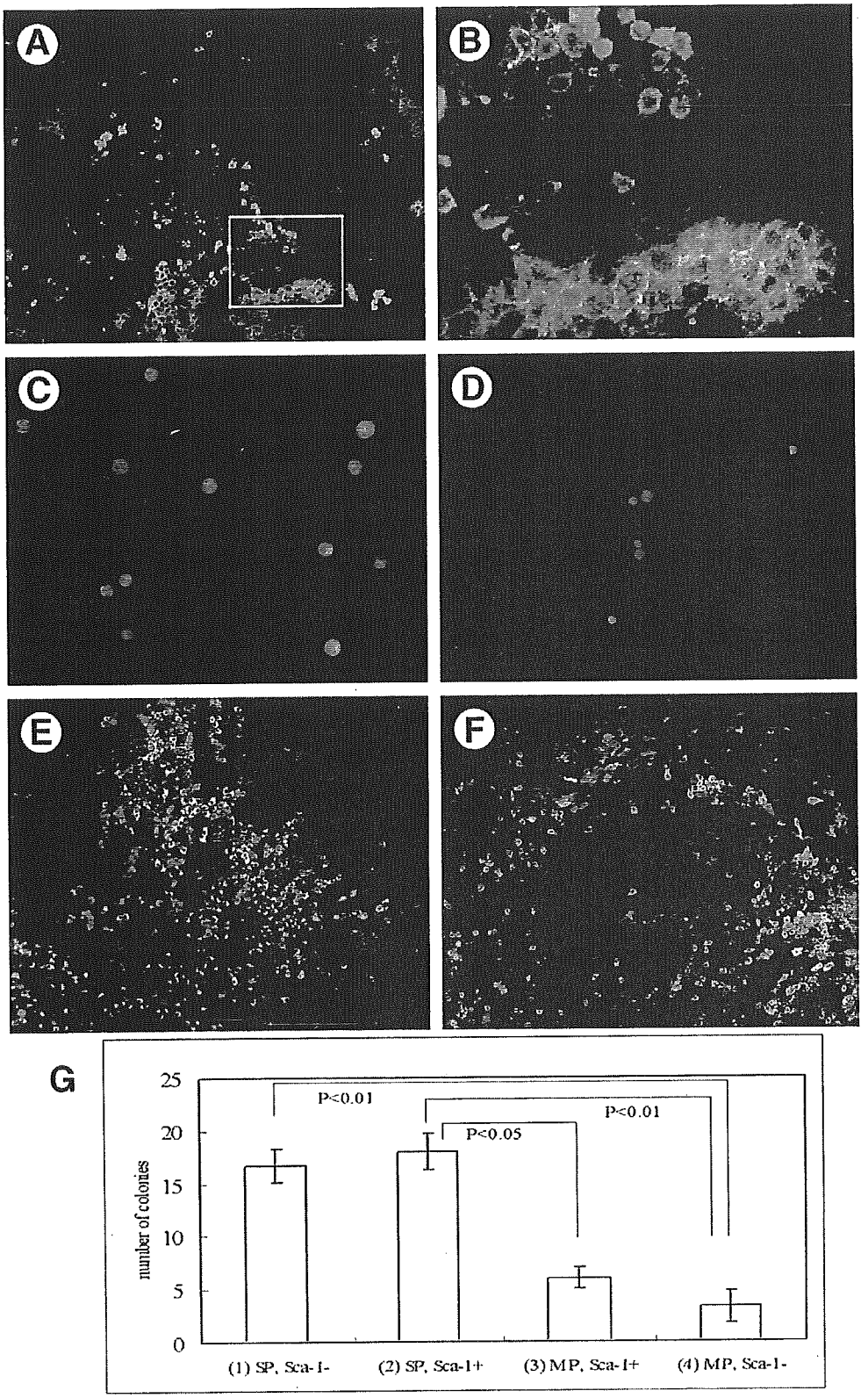

Figure 10. Analysis of the relationship among SP cells, Sca-1–positive cells, and AFP-positive cells. (*A*) Merged view of AFP-positive (*green*) and Sca-1–positive (*red*) cells. (*B*) Magnified areas surrounded by the white line in (*A*). AFP-positive cells were observed within a small cell population, whereas Sca-1–positive cells were slightly larger and mainly detected at the periphery of the small cell population. (*C* and *D*) The results of immunostaining with anti-AFP (*red*) in group 1 (*C*) and group 4 (*D*) are shown (nuclei are blue). Large colonies of each fraction contained (*E*) AFP-positive (*red*) and ALB-positive (*green*) cells and (*F*) AFP-positive (*green*) and CK7-positive (*red*) cells. (*G*) This graph shows the number of large colonies formed by each of 300 fractionated cells. The cells in groups 1 and 2 had a greater ability to form large colonies than those in groups 3 and 4 (original magnifications: *A*, *E*, and *F*, 100 ×; *C* and *D*, 200×).

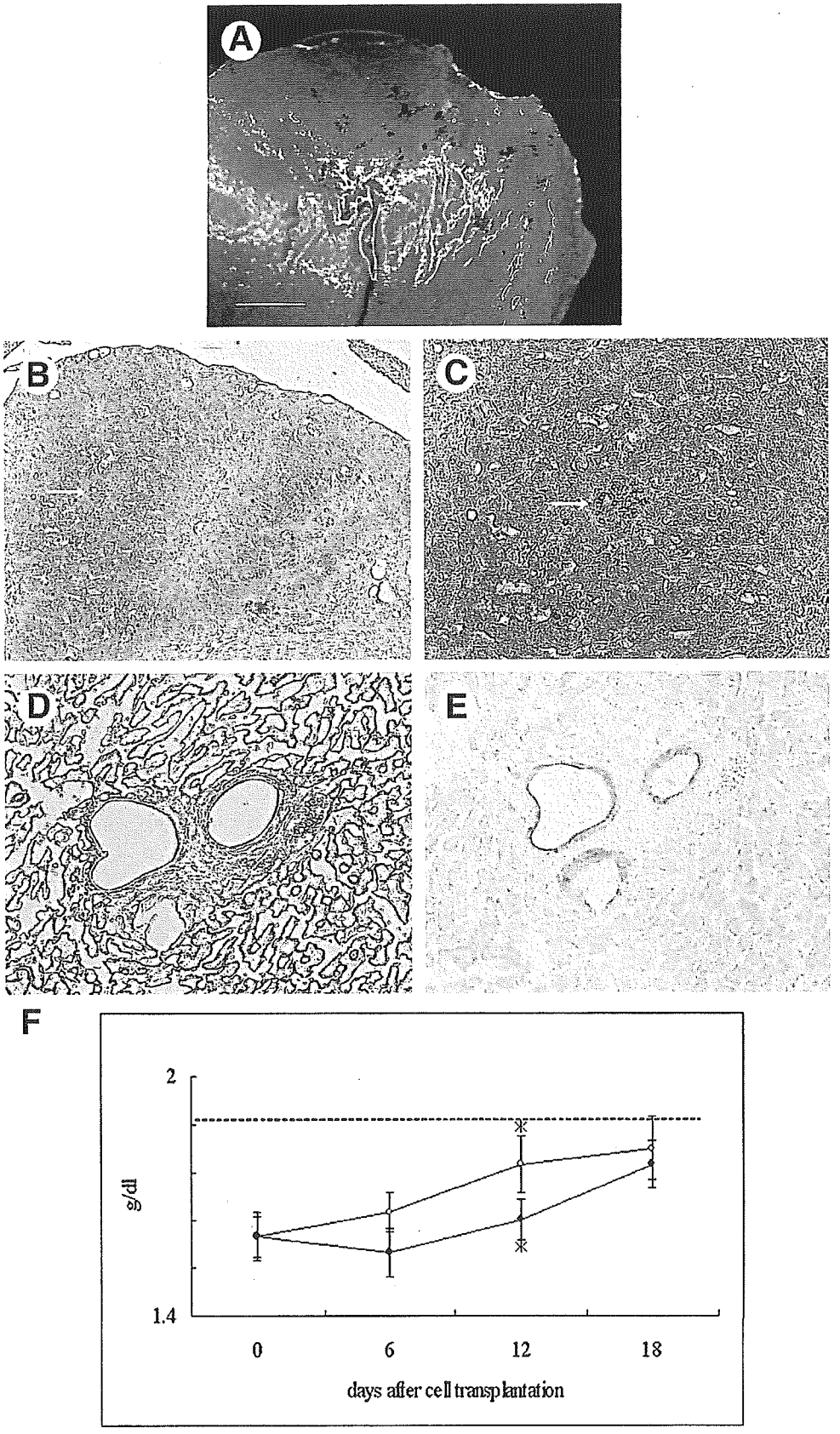

Figure 11. Analysis of recipient mice after cell transplantation and model of cultured cells. (*A*) β-gal–positive (*blue*) areas could be seen in the recipient livers (bar = 1 mm). (*B* and *C*) ALB (*brown*) and β-gal (*blue*) double-positive cells (*arrows*) and (*D*, X-gal staining; *E*, 3,3'-diaminobenzidine tetrahydrochloride staining) CK19 (*brown*) and β-gal (*blue*) double-positive cells could be seen. (*F*) Serum albumin levels in cell transplantation group increased more rapidly than those in the sham transplantation group. *Significant differences ($P < .05$) at each sample point; ○, cell transplantation group; ●, sham transplantation group; parallel dashed line, average level of normal mice. (*G*) Cultured cells were identified in a $CD34^-$, $Thy\text{-}1^-$, $c\text{-}kit^-$, $CD45^-$, $CD49f^+$ fraction. In this fraction, SP cells and Sca-1–positive cells were detected within the population of immature cells. SP cells were more immature than Sca-1–positive cells (original magnifications: *B*, 100×; *C–E*, 200×).